Check for updates

Received: 19 March 2024 | Revised: 21 June 2024 | Accepted: 19 August 2024

DOI: 10.1002/joc.8610

RESEARCH ARTICLE

International Journal of Climatology RMetS

Examining the evolution of extreme precipitation event using reanalysis and the observed datasets along the Western Ghats

Leena Khadke[1] | **Sachin Budakoti**[2] | **Akash Verma**[1] | **Moumita Bhowmik**[3] | **Anupam Hazra**[3]

[1]Department of Civil Engineering, Indian Institute of Technology Bombay, Mumbai, India

[2]Interdisciplinary Program in Climate Studies, Indian Institute of Technology Bombay, Mumbai, India

[3]Indian Institute of Tropical Meteorology, Ministry of Earth Sciences, Pune, India

Correspondence
Anupam Hazra, Indian Institute of Tropical Meteorology, Ministry of Earth Sciences, Pune 411008, India.
Email: hazra@tropmet.res.in

Abstract

In recent decades, India has witnessed an increase in the intensity, frequency, and spread of extreme weather events. The widespread increase in extreme precipitation over the Western Coast of India is a matter of great concern. The factors contributing to such devastating extreme precipitation remain unclear due to the variability present in meteorological and oceanic variables and associated large-scale circulations. Using reanalysis and observed datasets, we attempted to identify a combination of dynamic, thermodynamic, and cloud microphysics processes contributing to the anomalous precipitation from August 1 to 10, 2019 against its climatology. Our key findings highlight the crucial role of warm sea surface temperatures (anomaly >1.4°C), outgoing longwave radiation (anomaly $<-50\ \mathrm{W \cdot m^{-2}}$), and atmospheric temperature (anomaly over the ocean is >1.6°C) in enhancing the moisture-holding capacity of the atmosphere by almost 10%. This elevated moisture, propelled by intensified low-level winds (anomalies exceeding $4\ \mathrm{m \cdot s^{-1}}$), leads to a shift from ocean to land. Notably, we observe that vertical updrafts (anomalies $>-0.4\ \mathrm{m \cdot s^{-1}}$) contribute to increased atmospheric instability and moisture convergence. The presence of an ample amount of cloud hydrometeors, with anomalies surpassing $2.5 \times 10^{-4}\ \mathrm{kg \cdot kg^{-1}}$, establishes conditions conducive to sustained intense precipitation. Our findings deepen our understanding of the complex relationships between ocean and atmospheric dynamics, and wind patterns, and emphasize their pivotal influence on regional weather patterns and land surface hydrology.

KEYWORDS

atmospheric dynamics, ERA5, extreme precipitation, Western Ghats

1 | INTRODUCTION

In recent decades, the Earth's climate system has undergone unprecedented changes, primarily propelled by anthropogenic activities. The consequences of these changes have become increasingly evident in the form of extreme weather events. One of the most significant manifestations of climate change is the alteration of precipitation patterns and intensities, leading to an increase in the frequency and severity of extreme weather events

 © 2024 Royal Meteorological Society

(Bonebrake & Mastrandrea, 2010; Intergovernmental Panel on Climate Change (IPCC), 2023; Trenberth, 2011). The intensification of extreme precipitation events poses a significant risk of triggering socio-economic and environmental challenges. It is crucial to understand the underlying mechanisms and their interactions with a changing climate. (Deegala et al., 2023; Tabari, 2020; Tamoffo et al., 2023). As greenhouse gas emissions continue to rise, the Earth's climate system is experiencing shifts in atmospheric and oceanic circulation patterns, alterations in temperature gradients, and modifications in moisture distribution (Hay & Williams, 2023). These changes have been observed to influence the behaviour of precipitation systems, often leading to an amplification of intense rainfall events. However, the exact mechanisms governing this relationship remain multifaceted and vary across different geographical regions.

Over 70% of the annual rainfall in the Indian subcontinent is attributed to the monsoon season (Sebastian et al., 2023). This substantial precipitation plays a vital role in shaping the vegetation productivity of croplands throughout the nation (Verma et al., 2022). The Western Ghats, a mountain range along the southwestern coast of India, is one of the most affected regions, renowned for its ecological significance and contribution to regional climate patterns (Paul et al., 2018). In recent decades, the Western Ghats region has experienced shifts in its climatic conditions, evident by changes in temperature and precipitation patterns (Nikumbh et al., 2019; Varikoden et al., 2019). The extreme precipitation event that occurred in 2019 holds immense importance as it caused significant disruptions to local ecosystems and communities. Therefore, it is essential to investigate the complex relationship between atmospheric dynamics, thermodynamics, and cloud microphysics. The topography of the Western Ghats creates a distinct atmospheric circulation pattern, forcing moisture-laden air to ascend the mountain slopes (Hay & Williams, 2023; Rajendran et al., 2012). As the air rises, it cools and condenses, leading to cloud formation and precipitation (Khadke & Pattnaik, 2021). The complex interplay between large-scale atmospheric circulation, local wind patterns, and the region's topography contributes to the complexity of extreme precipitation events.

Outgoing longwave radiation (OLR) refers to the energy emitted from the Earth through longwave infrared radiation. This process is crucial for the Earth's energy balance, as it is one of the primary ways the planet loses heat to space. OLR is often used as a proxy for convection because regions with active convection tend to have thick, high-altitude clouds that block and absorb much of the outgoing infrared radiation and therefore, the low OLR is associated with the deep convection during monsoon (Chaudhari et al., 2010; Hazra et al., 2016). Deep convective areas typically have strong upward movements of warm, moist air, which can lead to cloud formation and precipitation (Chaudhari et al., 2010; Hazra et al., 2016). Clouds typically cover almost two-thirds of the global surface, modifying outgoing longwave radiation and reflecting more solar radiation than the underlying surface (Baker, 1997). The atmospheric hydrological cycle, latent heating, and cooling associated with clouds also modify atmospheric circulation (Baker, 1997). The vertically averaged air temperature between 200 and 600 hPa is known as tropospheric temperature (TT) (Goswami et al., 2006). Previous studies (e.g., Goswami et al., 2006; Goswami & Xavier, 2005) have established that the north–south TT difference is crucial for monsoon circulation. The amount of heat available in the troposphere can impact circulation and thermodynamic phase changes in the surrounding region.

Therefore, cloud microphysical processes, which are responsible for the latent heat release into the atmosphere for increasing tropospheric temperature, are the key factors to give feedback to large-scale monsoon dynamics. Microphysics is a fundamental aspect of precipitation processes, as the size, concentration, and characteristics of cloud particles influence the type and intensity of precipitation (Gao et al., 2016; Schmeller & Geresdi, 2019). As the atmosphere warms, alterations in cloud microphysics can lead to the generation of larger and more persistent cloud particles, potentially enhancing the tendency for extreme precipitation. Satellite observations indicate that about 40–50% of rainfall events over the Indian summer monsoon region originate from the melting of ice (Field & Heymsfield, 2015), underscoring the significant role of ice processes (Hazra et al., 2017). The composition of ice crystals and liquid droplets, considered as mixed-phase clouds, is important for Indian summer monsoon rainfall (Kumar et al., 2014; Rajeevan et al., 2013). Stratiform rain formation is closely associated with the formation of cloud condensate, particularly cloud ice and mixed-phase hydrometeors (Fu et al., 2011). The term cloud liquid water content (CLWC) signals the presence of water in the vertical column of the atmosphere. These liquid drops agglomerate to form large and heavy droplets, resulting in extreme precipitation. The term cloud ice water content (CIWC) denotes the concentration of ice available in the vertical column of the atmosphere.

In the context of extreme precipitation events, the presence of supercooled liquid water, ice particles, and ample of all hydrometeors (cloud, ice, snow, graupel, and rain droplets) within clouds can lead to enhanced riming and collision-coalescence processes, resulting in

10970088, 2024, 13, Downloaded from https://rmets.onlinelibrary.wiley.com/doi/10.1002/joc.8610 by University Of New South Wales, Wiley Online Library on [28/04/2025]. See the Terms and Conditions (https://onlinelibrary.wiley.com/terms-and-conditions) on Wiley Online Library for rules of use; OA articles are governed by the applicable Creative Commons License

more substantial raindrop formation and potentially intense rainfall rates. Climate change-induced alterations in cloud microphysics could contribute to the observed changes in precipitation patterns. Warming temperatures may influence the freezing level within clouds, affecting the distribution of ice crystals and snowflakes (Geresdi et al., 2005). Additionally, changes in aerosol composition and concentration due to human activities can impact cloud droplet nucleation and growth, potentially altering cloud properties and precipitation patterns. Investigating these microphysical processes is crucial for gaining insights into the mechanisms that drive extreme precipitation events and their relationship with climate change.

The study of any anomalous precipitation event replicates the interconnections between the atmospheric parameters. The continuous series of heavy rainfall in the past motivated us to understand the triggered mechanism of atmospheric scenarios because of rising global temperatures (Fischer & Knutti, 2015; Scoccimarro et al., 2013). The extreme precipitation event that occurred in August 2019 along the Southwest coast of India is an example of such episodes happening in India. The present research aims to understand the response of atmospheric dynamics, thermodynamics, and cloud microphysics during the extreme precipitation event (2019) given the climate change scenario along the coast of Gujarat, Maharashtra, Goa, Karnataka, and Kerala. Using the reanalysis, satellite, and observational datasets, our objectives are, (1) to investigate the atmospheric circulation patterns and topographical influences that contributed to the extreme precipitation event, (2) to examine the thermodynamic conditions that facilitated the intensification of the precipitation event, considering the influence of climate change-induced temperature shifts, (3) to explore the cloud microphysical processes that influenced precipitation enhancement during the event and their potential connections to changing atmospheric conditions. This study enhances our understanding of the complex interactions among atmospheric dynamics, thermodynamics, and cloud microphysics, specifically in the Western Ghats region. Our findings contribute valuable insights to improve regional modelling, risk assessment, and adaptive strategies for mitigating impacts from future extreme precipitation events.

2 | MATERIALS AND METHODS

2.1 | Study area

The varied topography of the western coastal states of India, including Gujarat, Maharashtra, Goa, Karnataka, and Kerala, plays a crucial role in shaping atmospheric circulations and precipitation patterns. The Western Ghats, running parallel to the Arabian Sea, significantly influences the regional climate. It acts as a barrier to the moisture-laden southwest monsoon winds, leading to orographic uplift and subsequent heavy rainfall on the windward side, particularly affecting Maharashtra, Goa, Karnataka, and Kerala. The steep slopes of the Western Ghats contribute to the enhancement of convective processes, leading to the formation of localized weather systems and influencing precipitation distribution. Figure 1 highlights the geographical area with complex topography as a study area for the present work.

The Western Ghats in India run parallel to the Arabian Sea coastline. The distance between the coast and the mountains varies along the length of the Western Ghats, typically ranging from 30 to 50 km (UNESCO World Heritage Centre, 2024). These mountains span across the states of Kerala, Tamil Nadu, Karnataka, Goa, Maharashtra, and Gujarat. This proximity is not consistent throughout the entire stretch of the Western Ghats due to variations in terrain and geography across different regions. Gujarat, which is characterized by the diverse landscapes including coastal areas and the arid Rann of Kutch, is experiencing unique atmospheric circulations. The Gulf of Khambhat and the Arabian Sea influence the state's climate, with the proximity to water bodies contributing to variations in temperature and precipitation. The complex topography of the region, from the coastal plains to the Western Ghats, results in diverse microclimates. This complex interplay between topography and geographic features contributes to the dynamic and varied atmospheric circulations and precipitation patterns observed across Gujarat, Maharashtra, Goa, Karnataka, and Kerala, influencing the overall climate of the western coastal region.

2.2 | Datasets used and methodology

The present study used 35 years of climatological data starting from July 27, 1984 to August 10, 2018 against July 27 to August 10, 2019. We also used the fifth-generation ERA5 reanalysis product of the European Centre for Medium-Range Weather Forecasts (ECMWF) contains the global climate reanalysis for the same period (https://cds.climate.copernicus.eu/#!/search?text=ERA5&type=dataset). The available ERA5 data used a 4D-Var data assimilation scheme which contains vertically 137 hybrid pressure/sigma levels. The present study used ERA5 reanalysis hourly on pressure levels with 37 pressure levels (Hersbach et al., 2020) and single levels datasets with a spatial resolution of 0.25°. We used atmospheric and ocean variables such as temperature

10970088, 2024, 13, Downloaded from https://rmets.onlinelibrary.wiley.com/doi/10.1002/joc.8610 by University Of New South Wales, Wiley Online Library on [28/04/2025]. See the Terms and Conditions (https://onlinelibrary.wiley.com/terms-and-conditions) on Wiley Online Library for rules of use; OA articles are governed by the applicable Creative Commons License

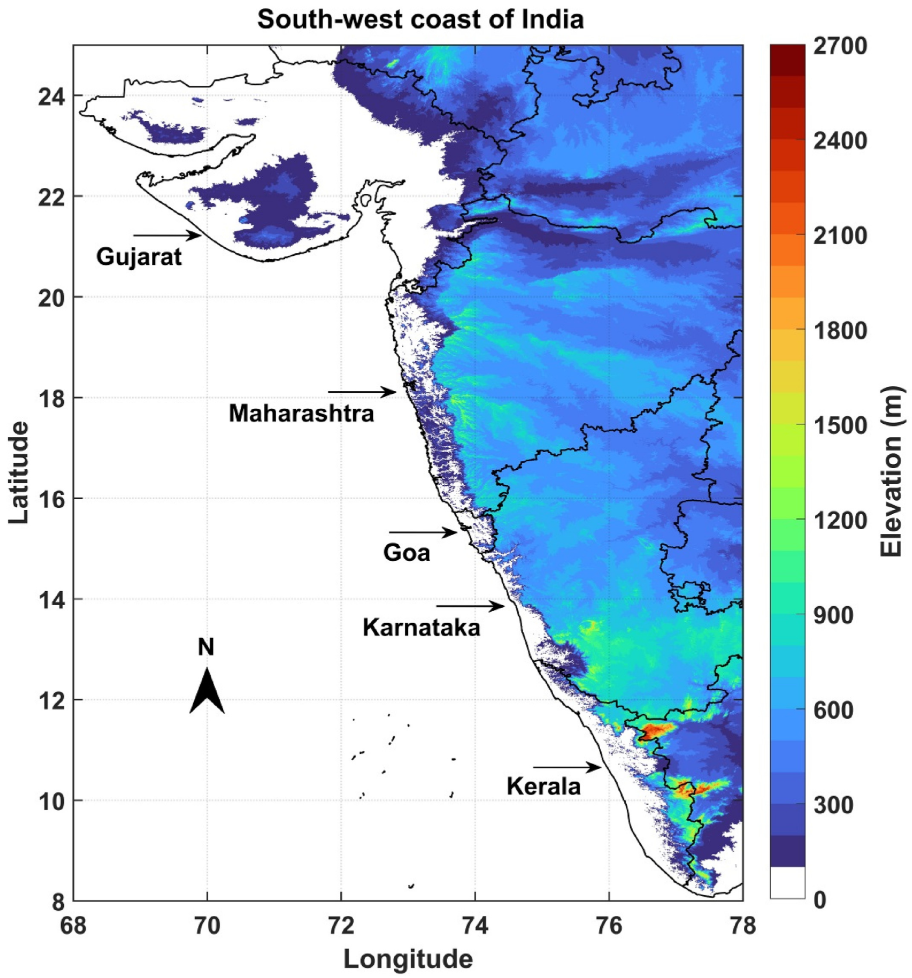

FIGURE 1 Illustration of the geographical area considered in the present work. DEM data from Shuttle Radar Topography Mission (SRTM) of 30 m resolution available at https://dwtkns.com/srtm30m/ has been used. [Colour figure can be viewed at wileyonlinelibrary.com]

(TA), relative humidity (RH), U and V components of wind, vertical velocity (VV), specific cloud liquid water content (CLWC), specific cloud ice water content (CIWC), specific rainwater content (RWC), specific snow water content (SWC), assessed from ERA5 hourly data on pressure levels for the same period (1984–2019). We aggregated hourly scale datasets to daily temporal scale.

The present study used India Meteorological Department (IMD) rainfall data available on a spatial resolution of $0.25^\circ \times 0.25^\circ$ (Pai et al., 2014; https://imdpune.gov.in/cmpg/Griddata/Rainfall_25_Bin.html). We have used the IMD rainfall observations to create the spatial plots of rainfall from August 1 to 10 as well as the probability distribution (PDFs). We used the National Oceanic and Atmospheric Administration's (NOAA) $0.25^\circ \times 0.25^\circ$ daily optimum interpolation Sea Surface Temperature (OISST) dataset version 2.0 (https://downloads.psl.noaa.gov/Datasets/noaa.oisst.v2.highres/). The data obtained from the National Oceanic and Atmospheric Administration (NOAA) Climate Data Record (CDR) of Daily Outgoing Longwave Radiation (OLR), version 1.2 is used to analyse the OLR over the study region (https://www.ncei.noaa.gov/data/outgoing-longwave-radiation-daily/access/). The data is produced as daily mean upward longwave flux measured at the top of the atmosphere with a spatial resolution of $1^\circ \times 1^\circ$. The detailed methodology adopted for the present work is illustrated in Figure 2.

3 | RESULTS AND DISCUSSION

3.1 | Heavy rainfall event

The present study focuses on the underlying mechanism behind the extreme rainfall event that occurred in August, affecting consecutively the Southwest coast of India, covering the states of Gujarat, Maharashtra, Goa, Karnataka, and Kerala. The spatial distribution of rainfall, as recorded by the India Meteorological Department (IMD), is shown in Figure 3a–j. On August 1 (Figure 3a), Gujarat witnessed rainfall in a few locations. After this, between August 3 and 5 (Figure 3c–e), the coastal region of Maharashtra encountered heavy rainfall with a magnitude >160 mm, which may be the potential cause of the flood situation. Following closely, from August 6 to

10970088, 2024, 13, Downloaded from https://rmets.onlinelibrary.wiley.com/doi/10.1002/joc.8610 by University Of New South Wales, Wiley Online Library on [28/04/2025]. See the Terms and Conditions (https://onlinelibrary.wiley.com/terms-and-conditions) on Wiley Online Library for rules of use; OA articles are governed by the applicable Creative Commons License

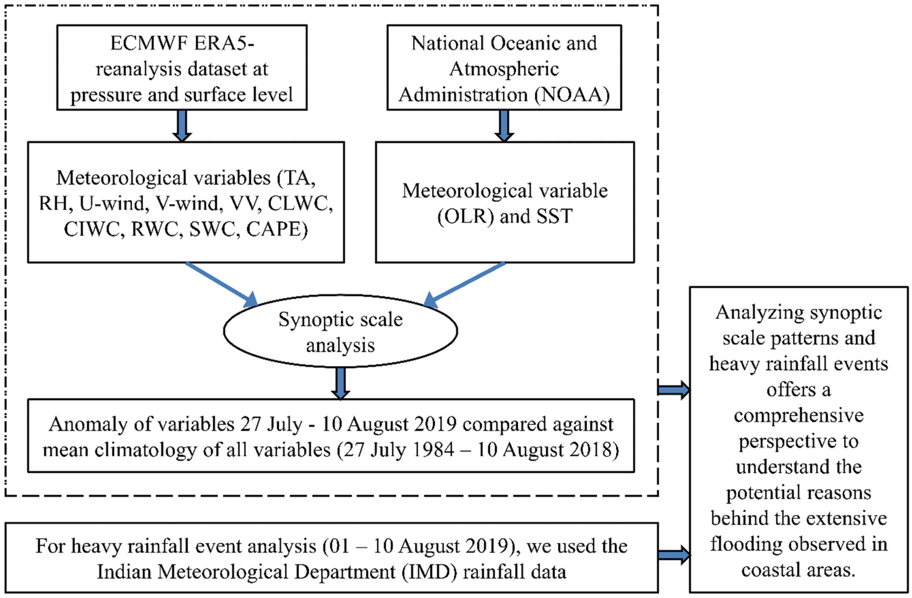

FIGURE 2 Methodology and datasets used in the present study. [Colour figure can be viewed at wileyonlinelibrary.com]

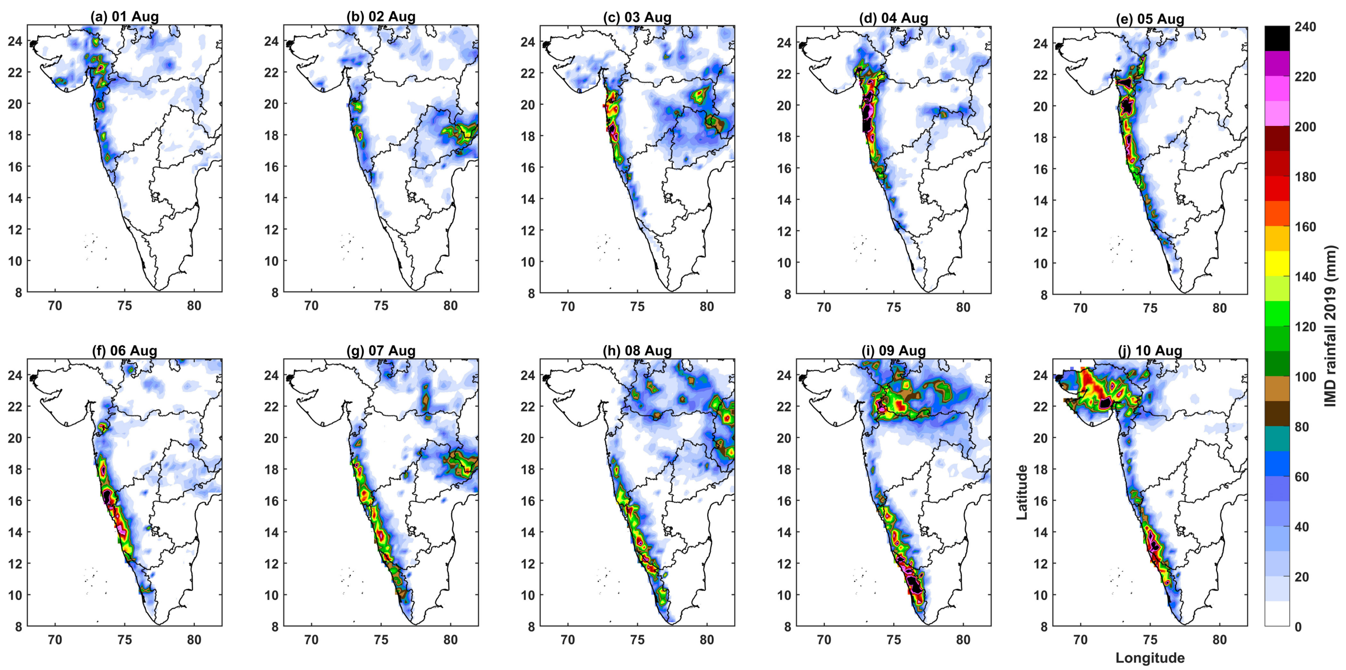

FIGURE 3 IMD rainfall (mm) observed during August 1–10, 2019 along the southwest coast of India. [Colour figure can be viewed at wileyonlinelibrary.com]

10 (Figure 3f–j), Goa, Karnataka, and Kerala experienced continuous and intense rainfall, which indicates the downward propagation of heavy rain bands along the coastal regions. On August 9th and 10th, the state of Gujarat also witnessed severe rainfall and flooding, causing chaos in the affected areas. This extreme precipitation was also attributed to various meteorological factors that played a role in its occurrence. On August 9th, Kerala experienced very heavy rainfall exceeding 180 mm, resulting in widespread flooding across the coastal region (Figure 3i).

The dynamic and varied patterns in rainfall locations, distribution, and intensity mirror the unique behaviour of atmospheric phenomena. This behaviour is the outcome of a complex interplay of diverse atmospheric and oceanic factors, emphasizing the complex nature of the climatic events in the southwest part of the Indian subcontinent. We accessed the convective available potential energy (CAPE) and total precipitation (*P*) dataset from ERA5 hourly data on single levels from 1940 to the present. The extreme rainfall event occurred from August

10970088, 2024, 13, Downloaded from https://rmets.onlinelibrary.wiley.com/doi/10.1002/joc.8610 by University Of New South Wales, Wiley Online Library on [28/04/2025]. See the Terms and Conditions (https://onlinelibrary.wiley.com/terms-and-conditions) on Wiley Online Library for rules of use; OA articles are governed by the applicable Creative Commons License

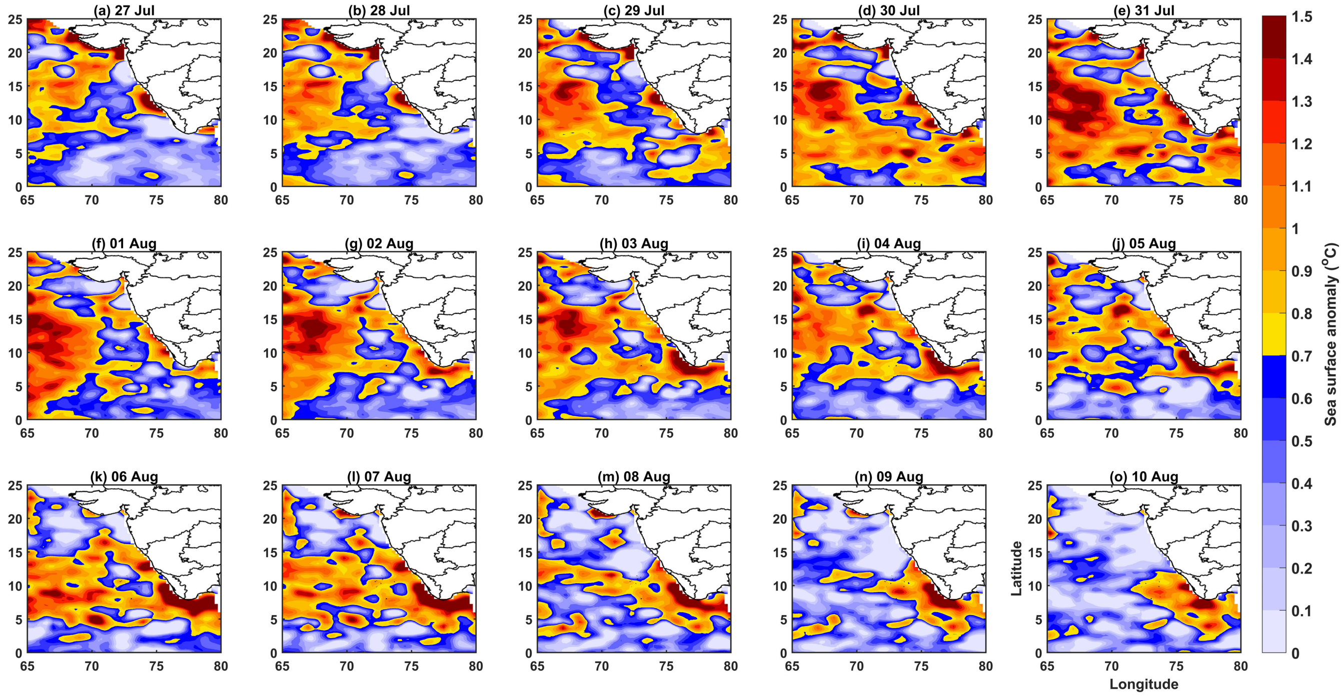

FIGURE 4 Sea surface temperature (SST) anomaly (°C) spanning from July 27 to August 10. [Colour figure can be viewed at wileyonlinelibrary.com]

1st to 10th along the southwest coast of India. Throughout this period, the Madden–Julian Oscillation (MJO) remained inactive, as evidenced by the absence of MJO signals in the Indian Ocean, as shown in Figure S1, Supporting Information. Rainfall anomalies were predominantly clustered over the landmass and along the coastal regions and not on the ocean (Figure S1). A study conducted in Indonesia from January 27th to 31st, 2021 for hail events, observed that large-scale circulations, such as the MJO, did not influence weather patterns in the region (Auliya & Mulya, 2022). Therefore, the effect of MJO during the extreme precipitation event (the precipitation anomaly as shown in Figure S1), we could not find signals of large-scale circulations during the event duration.

3.2 | Ocean–atmosphere interactions

Figure 4 shows the positive SST anomaly (°C) obtained from the climatological mean spanning 35 years (1984–2018) and 2019, covering the period from July 27 to August 10. A continuous rise in ocean temperature is observed in comparison with its climatological mean over the Arabian Sea from July 27 to July 31, which subsequently triggered the generation of moisture in the atmosphere (Figure 4a–e). In the second row (Figure 4f–j), the Arabian Sea shows a consistently warm ocean temperature (anomaly >1.4°C), ensuring a continuous supply of moisture from the ocean. In line with this, studies have documented that the Arabian Sea maintains a persistent warm pool in the region, which acts as a precursor for precipitation over the Indian subcontinent (Li & Yang, 2017; Vinayachandran et al., 2007). In the third row (Figure 4k–o), SST anomalies are very high near the coast of Kerala which supplied the continuous moisture for evolution of extreme precipitation over the region. We observe the continuous downward shift in high SST anomaly. Initially, on August 1, the spatial distribution and intensity of the SST anomaly are notably high near the Gujarat coast. Subsequently, the SST location shifts from a higher latitude to a lower latitude.

We have used the daily climatology of SST to estimate the anomalies. The daily SST climatology exhibits minimal noise as shown in Figure S3 as below. Therefore, we can conclude that the features in Figure 4 will not be affected by climatological noise. In August 2019, the western coast of India experienced extreme rainfall events, leading to widespread flooding and significant damage. This extreme weather event was influenced by a positive Indian Ocean Dipole (IOD) phase. As evident from Figure 4, the sea surface temperature anomalies are significantly high (>1.4°C) in the western Indian Ocean. This increased moisture availability and atmospheric instability, contributing to the intense and prolonged rainfall experienced along the western coast, which exceeded normal monsoon patterns.

10970088, 2024, 13, Downloaded from https://rmets.onlinelibrary.wiley.com/doi/10.1002/joc.8610 by University Of New South Wales, Wiley Online Library on [28/04/2025]. See the Terms and Conditions (https://onlinelibrary.wiley.com/terms-and-conditions) on Wiley Online Library for rules of use; OA articles are governed by the applicable Creative Commons License

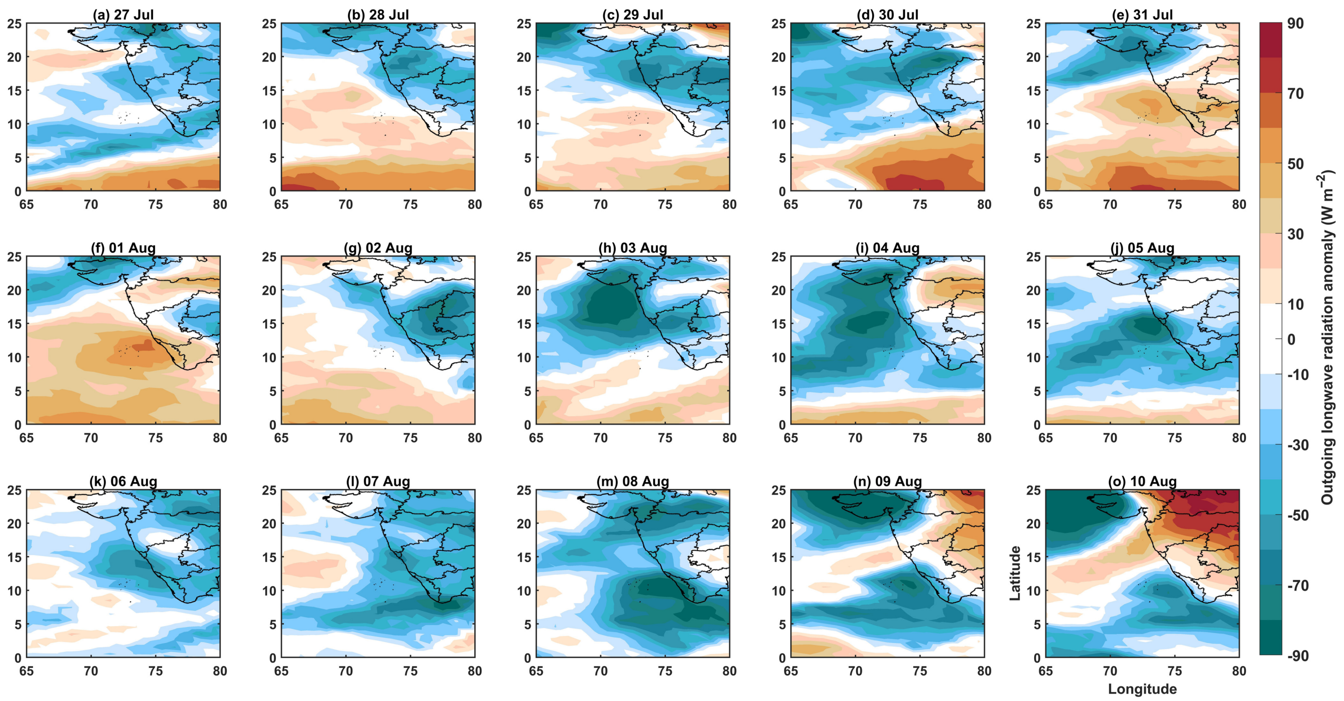

FIGURE 5 Outgoing longwave radiation (OLR) anomaly (W·m^{-2}) spanning from July 27 to August 10. [Colour figure can be viewed at wileyonlinelibrary.com]

The spatial distribution of the outgoing longwave radiation (OLR) anomaly is illustrated in Figure 5a–o. The OLR refers to the thermal radiation emitted by the Earth's surface and atmosphere into space. To measure OLR, a satellite detects the cloud top temperature or the surface temperature of the Earth when there are no clouds present. It shows the negative OLR anomaly values over both ocean and land areas, indicating the regions of intense large-scale convection associated with the monsoon. Simultaneously, low OLR anomalies signify increased heat absorption by ocean water, potentially leading to elevated SST As a reference; we have added the 35-year climatology of OLR in Figure S4. Budakoti and Singh (2023) investigated extreme rainfall events over the northwestern Himalayan region using the convective permitting Weather Research and Forecasting (WRF) model and remotely sensed observations. The findings suggest that during extreme rainfall conditions, there is a decrease in the magnitude of OLR by approximately 90–100 W·m^{-2} over potentially affected locations with extreme rainfall events (Budakoti & Singh, 2023). In the first row of Figure 5a–d, prominent convection is evident over the land region. This intense convection centered on the Gujarat area initiated rainfall on August 1. Subsequently, on August 3, a highly intense convective mechanism occurred near the Maharashtra coast, likely contributing to heavy rainfall during August 3–5 (Figure 5h–j) along the Maharashtra state coast. Between August 6–8 (Figure 5k–m), heavy convection was observed over the Western Ghats. However, starting from August 9 (Figure 5n), the strength of convection diminished.

The temperature serves as the thermodynamic component within the atmosphere. The temperature gradient is the fundamental driver of heat exchange in the atmosphere. Figure 6 illustrates the positive temperature anomaly averaged between 900 and 800 hPa in the atmosphere. The strong Land-Ocean lower-level temperature gradient started developing on August 1 (Figure 6a), which subsequently evolved and sustained till August 9 (Figure 6i) and then weakened on August 10 (Figure 6j). During the period of August 3–5, Maharashtra experienced heavy rainfall, and this developing temperature gradient supports the mechanism of rainfall formation. This mechanism is also applicable to the Goa, Karnataka, and Kerala regions. The pronounced temperature gradient as compared to its climatology, likely played a significant role in transporting moisture from the ocean to the land, contributing to the anomaly in the rainfall event. Several studies suggest that increasing land–sea thermal gradient between land and sea enhances the moisture transport from the ocean to the Indian subcontinent (Gadgil et al., 2019; Lau & Kim, 2017; Wu et al., 2022).

Figure 7 illustrates the percentage of positive anomalies in lower-level relative humidity (RH), averaging over the atmospheric pressure range of 900–800 hPa. The

10970088, 2024, 13, Downloaded from https://rmets.onlinelibrary.wiley.com/doi/10.1002/joc.8610 by University Of New South Wales, Wiley Online Library on [28/04/2025]. See the Terms and Conditions (https://onlinelibrary.wiley.com/terms-and-conditions) on Wiley Online Library for rules of use; OA articles are governed by the applicable Creative Commons License

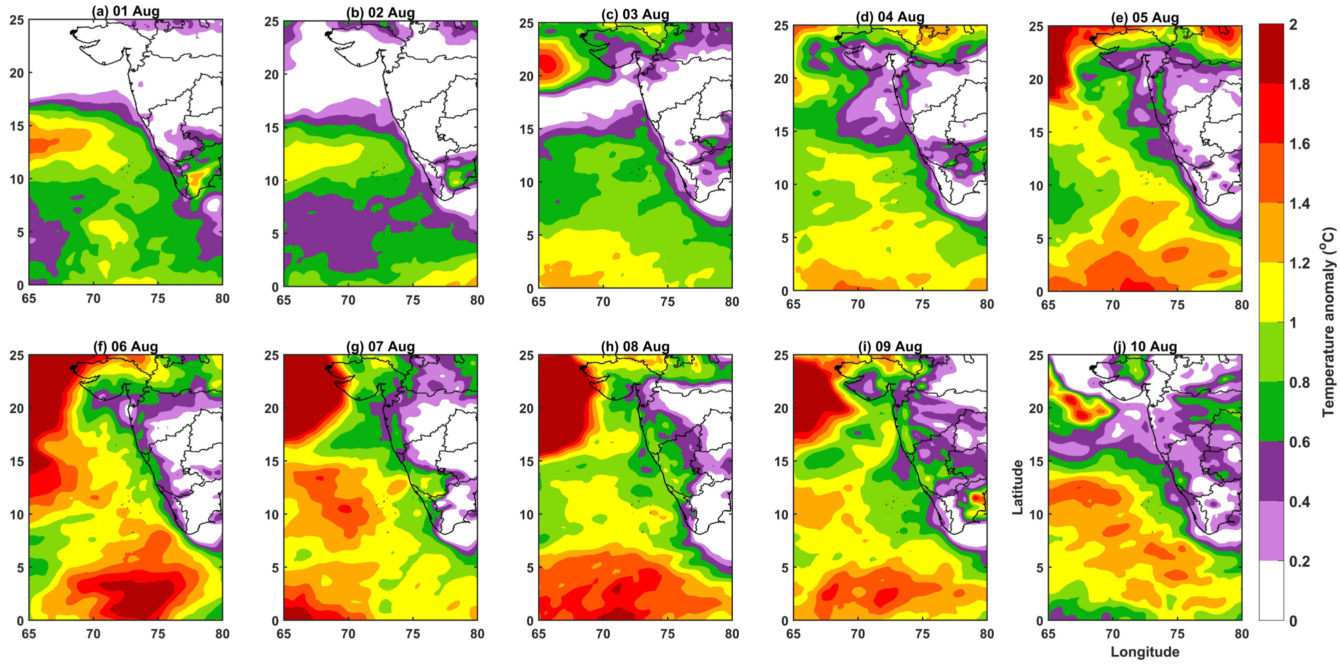

FIGURE 6 Air temperature (TA, unit:°C) anomaly averaged between 900 and 800 hPa spanning from August 1 to 10. [Colour figure can be viewed at wileyonlinelibrary.com]

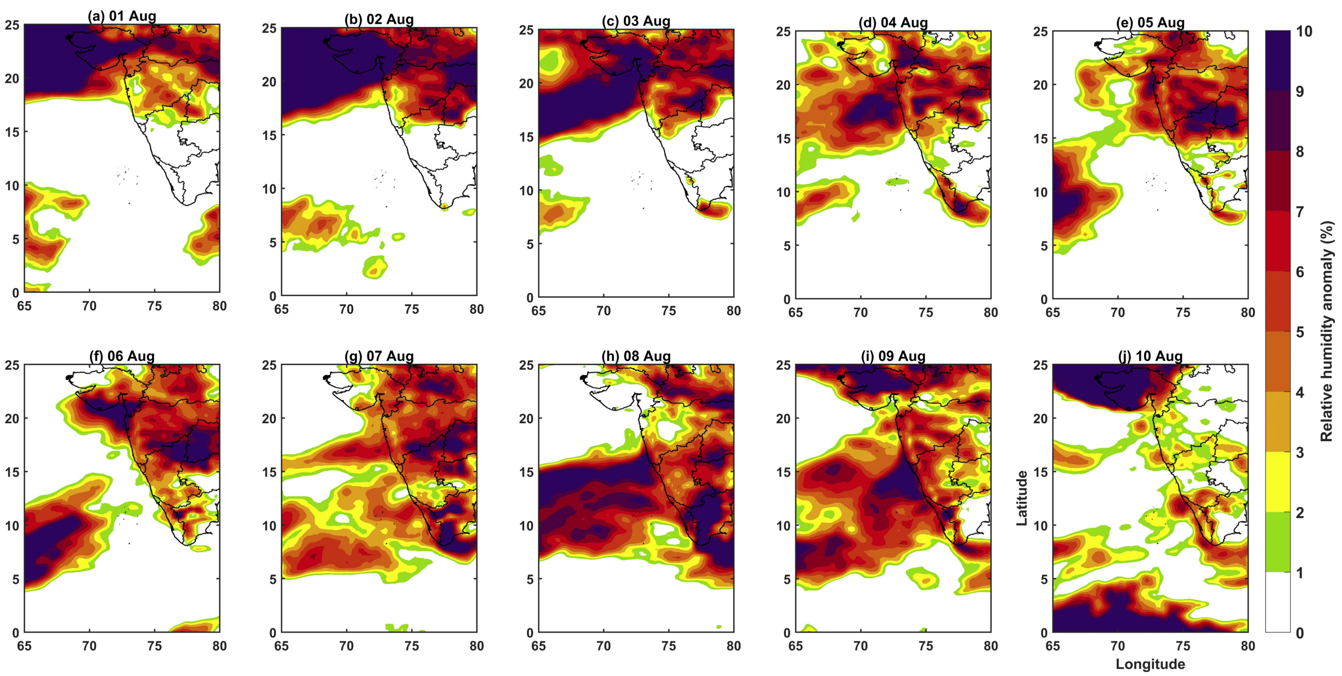

FIGURE 7 Relative humidity anomaly between averaged 900–800 hPa (%) spanning between August 1 and 10. [Colour figure can be viewed at wileyonlinelibrary.com]

pronounced lower-level temperature gradient that has emerged may have played a crucial role in transporting moisture over the land region. Throughout the progression of the event from Gujarat to Kerala between August 1st and 10th, there is a noticeable shift in the patches of RH from north to south. Notably, there is a significant increase in RH, with the atmosphere containing up to 10% more humidity compared to its climatological average over the past 35 years. Furthermore, on August 8th (as depicted in Figure 7h), the spatial coverage of a high

10970088, 2024, 13, Downloaded from https://rmets.onlinelibrary.wiley.com/doi/10.1002/joc.8610 by University Of New South Wales, Wiley Online Library on [28/04/2025]. See the Terms and Conditions (https://onlinelibrary.wiley.com/terms-and-conditions) on Wiley Online Library for rules of use; OA articles are governed by the applicable Creative Commons License

10970088, 2024, 13, Downloaded from https://rmets.onlinelibrary.wiley.com/doi/10.1002/joc.8610 by University Of New South Wales, Wiley Online Library on [28/04/2025]. See the Terms and Conditions (https://onlinelibrary.wiley.com/terms-and-conditions) on Wiley Online Library for rules of use; OA articles are governed by the applicable Creative Commons License

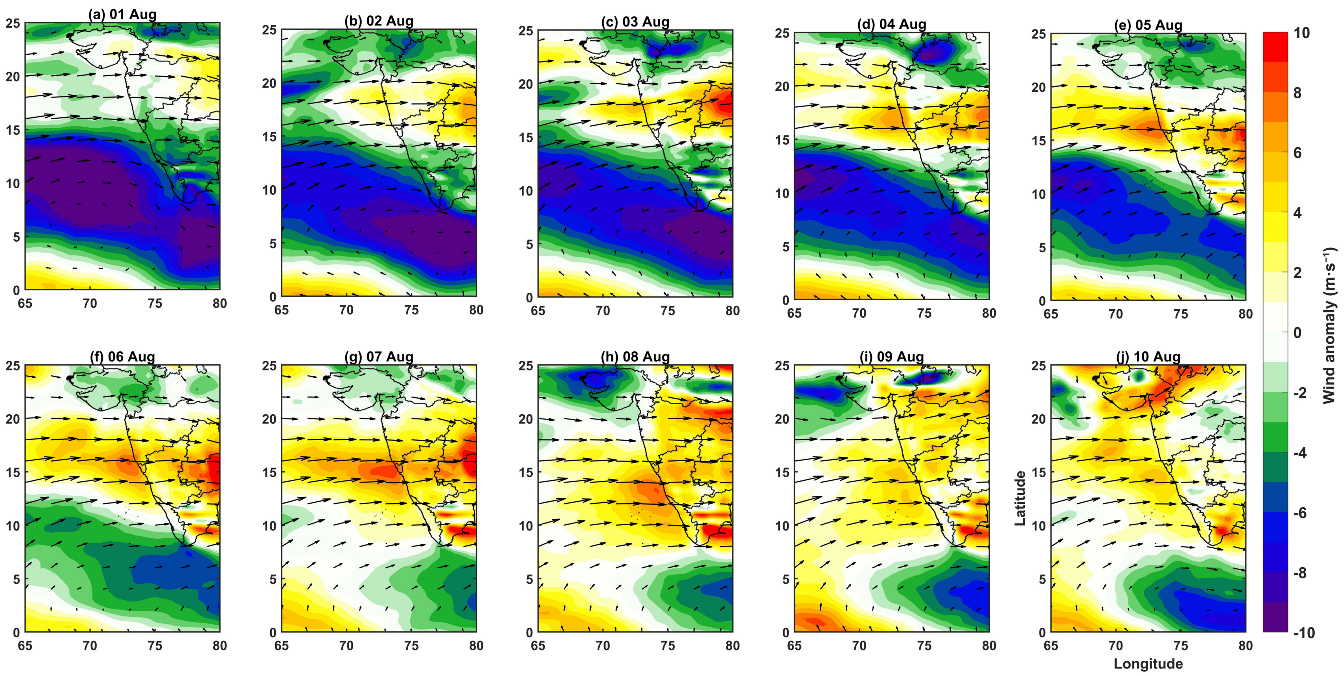

FIGURE 8 Wind anomaly at 850 hPa ($m \cdot s^{-1}$) spanning between August 1 and 10. The colour bar indicates the anomalies of wind strength, while the arrow length signifies wind flow/directions. [Colour figure can be viewed at wileyonlinelibrary.com]

percentage RH is at its peak, concentrated between latitudes 5°N and 17°N. This indicates substantial atmospheric moisture content during this period. The observed changes in RH patterns provide valuable insights into the dynamic behaviour of humidity levels during the specified timeframe.

The spatial distribution of wind anomalies at 850 hPa is illustrated in Figure 8a–j. The 850 hPa pressure level is chosen because it represents the maximum transport of moisture from the adjacent oceans towards the Indian landmass at this specific pressure level (Shahi et al., 2021). The arrows in the figure depict the U and V wind components recorded from 1 to 10 August 2019. The colour bar indicates the positive anomaly of wind strength, while the length of the arrows represents wind flow. Notably, a substantial positive wind anomaly is observed, indicating a high wind flow from the ocean to the land within the 10°–24°N latitude range (Figure 8a–e). Throughout August 6–10, there is a noticeable expansion in the spatial coverage of the positive wind anomaly. It extends from 11°N to 25°N latitude to 0°N to 25°N latitude, encompassing the entire southwest coast of India (Figure 8f–j). This expansion signifies a broader influence of the wind anomaly, suggesting a shift or intensification of atmospheric patterns during this period.

During the extreme rainfall events in August 2019, the stronger low-level jets (LLJs) over the Arabian Sea (Figure 8) are effectively transporting ample of moisture from the ocean to the Indian landmass (Figure 7). As the stronger LLJs carried more moist air towards the Western Ghats, the mountain helps for the orographic lifting and forcing the moist air to rise. This orographic lifting caused the moisture-laden air to cool and condense rapidly, leading to intense and prolonged rainfall in the region. The strong LLJs created zones of atmospheric convergence along the western coast, where the airflows collided and were forced upward. This convergence, combined with the inherent instability of the atmosphere due to the warm sea surface temperatures associated with the positive Indian Ocean Dipole (IOD), led to vigorous convective activity and extreme rainfall. The continuous supply of moisture through LLJs sustained heavy rainfall over an extended period. The combined effects of the LLJs and the positive IOD phase were crucial in amplifying the monsoon dynamics, resulting in the extreme rainfall events along the western coast of India.

The persistent strong westerly wind anomalies during Boreal Summer Intra-Seasonal Oscillation (BSISO) (July and August months) are significantly responsible for the heavy rainfall events due to the interaction between dynamics and cloud microphysics. The strong wind anomaly or cross-equatorial flow over the Arabian Sea helps to produce more sea salt by bubble burst, which can act as giant condensation nuclei (GCCN) and have an impact on the precipitation through rain embryo formation (microphysical processes). This interaction between dynamical (wind) and cloud microphysics

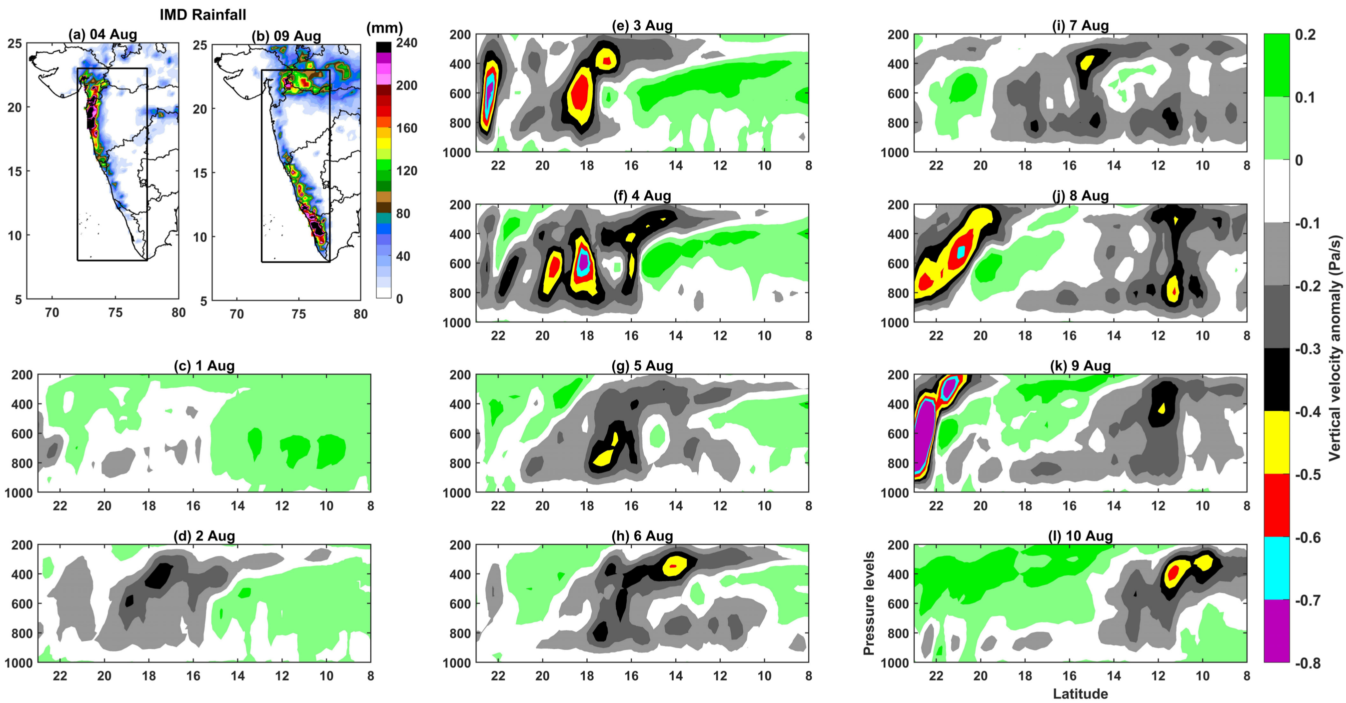

FIGURE 9 (a, b) The IMD rainfall of August 4 and 9, 2019. (c–l) Vertical velocity anomaly (Pa/s) plotted along latitude and pressure level, average over longitude in the selected box 72°–77.5°E in longitude and 8°–23°N in latitude. [Colour figure can be viewed at wileyonlinelibrary.com]

(cloud hydrometeors) is very specific over the particular region of interest. The formation of cloud hydrometeors at lower levels are conducive over the particular region due to the presence of ample sea salt, which can act as rain embryos. The heavy rainfall over other regions during BSISO might be very general and more driven by dynamics.

Figure 9c–l illustrates the anomaly in VV over the Western Ghats, with negative values indicating upward motion of the air parcel. To analyse this phenomenon, a specific geographical box ranging from 72°E to 77.5°E in longitude and 8°N to 23°N in latitude was selected. The longitudinal average of VV was then considered along this box to observe patterns over time (Figure 9c–l). Simultaneously, Figure 9c–l displays a notable increase in the amplitude of negative VV, signalling the upward movement of air parcels. Examining the IMD gridded rainfall for August 4 and 9, 2019, in Figure 9a,b, an association emerges with the development of the positive VV anomaly. Starting on August 1 (Figure 9c), this anomaly progressed from higher latitudes towards lower latitudes until August 10 (Figure 9l). Notably, on August 3–4 (Figure 9e,f), an intense VV between 23°N and 17°N latitude was observed, encompassing areas of South Gujarat and Maharashtra. Subsequently, this VV patch shifted to the region of Goa and Karnataka between 18°N and 11°N latitude (Figure 9g–i). In the final phase, from August 8–10 (Figure 9j–l), VV dominance occurred between 15°N and 8°N latitude, covering parts of Karnataka and Kerala. These findings suggest a dynamic spatiotemporal evolution of VV anomalies, showcasing distinct patterns and shifts over the selected Western Ghats region during the specified timeframe. In a modelling study, Raju et al. (2015) found that robust upward motion is attributed to a moist and unstable atmosphere, characterized by a significant VV (extending up to 100 hPa) linked to intense precipitation.

While VV serves as an indicator of the vertical movement of air parcels, CAPE is a crucial metric measuring the energy available for convection within the atmosphere. In Figure 10a–j, the elevated CAPE anomaly is indicative of the substantial energy reservoir present in the atmosphere. Simultaneously, Figure 9c–l displays a notable increase in VV, signalling the upward movement of air parcels. This simultaneous occurrence of high VV and elevated CAPE implies the lifting of air parcels, fostering the development of vertical motion and potentially contributing to the formation of convective clouds and storms. Notably, the observed CAPE anomalies commenced their ascent on August 1st, reaching a peak between August 4th and 9th, 2018, along the southwest coast of India. The increased instability of the atmosphere attributed to the increased CAPE values has significantly intensified convective activity over the region

10970088, 2024, 13, Downloaded from https://rmets.onlinelibrary.wiley.com/doi/10.1002/joc.8610 by University Of New South Wales, Wiley Online Library on [28/04/2025]. See the Terms and Conditions (https://onlinelibrary.wiley.com/terms-and-conditions) on Wiley Online Library for rules of use; OA articles are governed by the applicable Creative Commons License

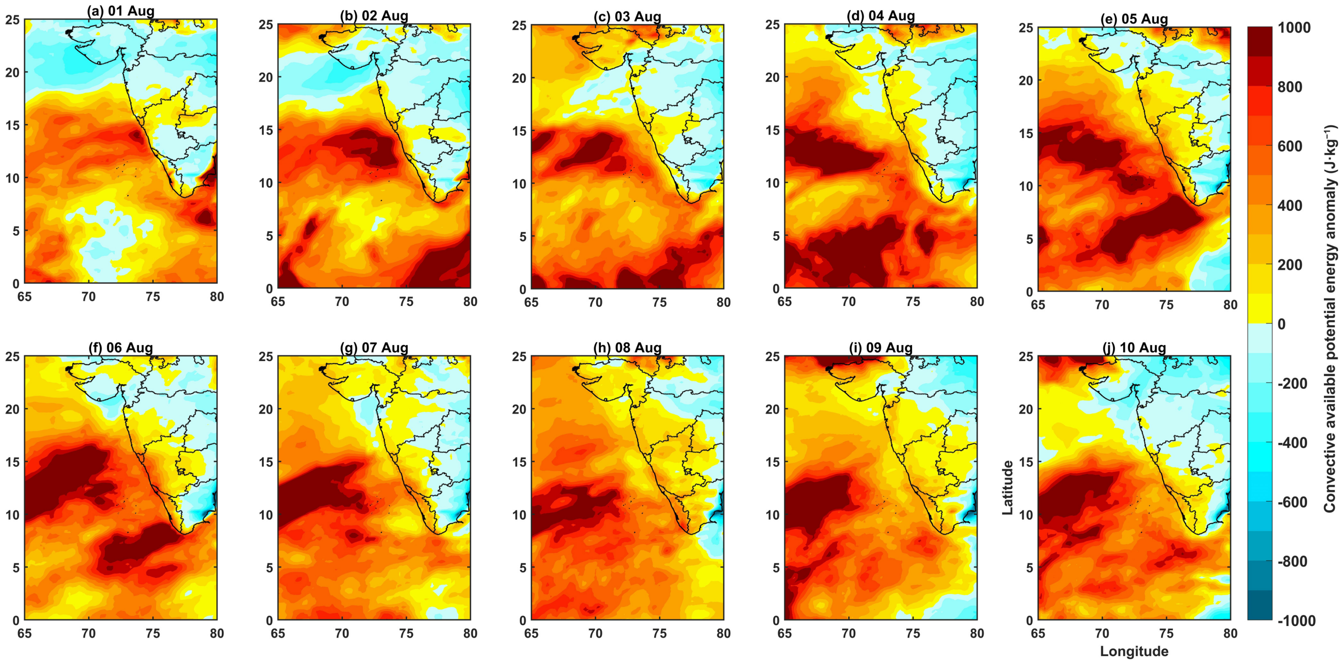

FIGURE 10 Convective available potential energy (CAPE) anomalies during August 1–10. Positive values indicate the higher instability of the atmosphere. [Colour figure can be viewed at wileyonlinelibrary.com]

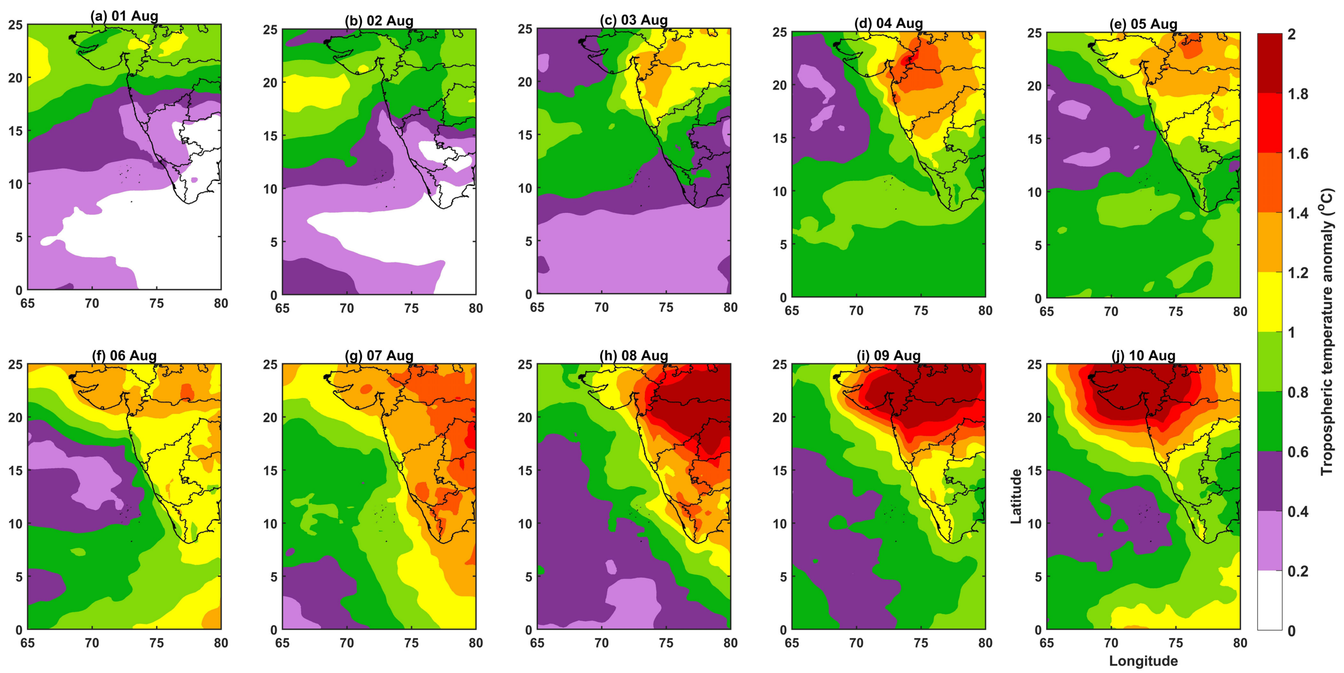

FIGURE 11 Tropospheric temperature (TT) anomaly between 600 and 200 hPa (°C). [Colour figure can be viewed at wileyonlinelibrary.com]

(Lee & Frisius, 2018; Murugavel et al., 2012). These conditions have created a conducive environment for meteorological phenomena, resulting in extreme precipitation during this period. In essence, the synchronicity of elevated VV and CAPE levels during this timeframe suggests a dynamic interplay that has influenced atmospheric instability, ultimately contributing to the heightened convective processes and consequential meteorological events, particularly extreme precipitation.

10970088, 2024, 13, Downloaded from https://rmets.onlinelibrary.wiley.com/doi/10.1002/joc.8610 by University Of New South Wales, Wiley Online Library on [28/04/2025]. See the Terms and Conditions (https://onlinelibrary.wiley.com/terms-and-conditions) on Wiley Online Library for rules of use; OA articles are governed by the applicable Creative Commons License

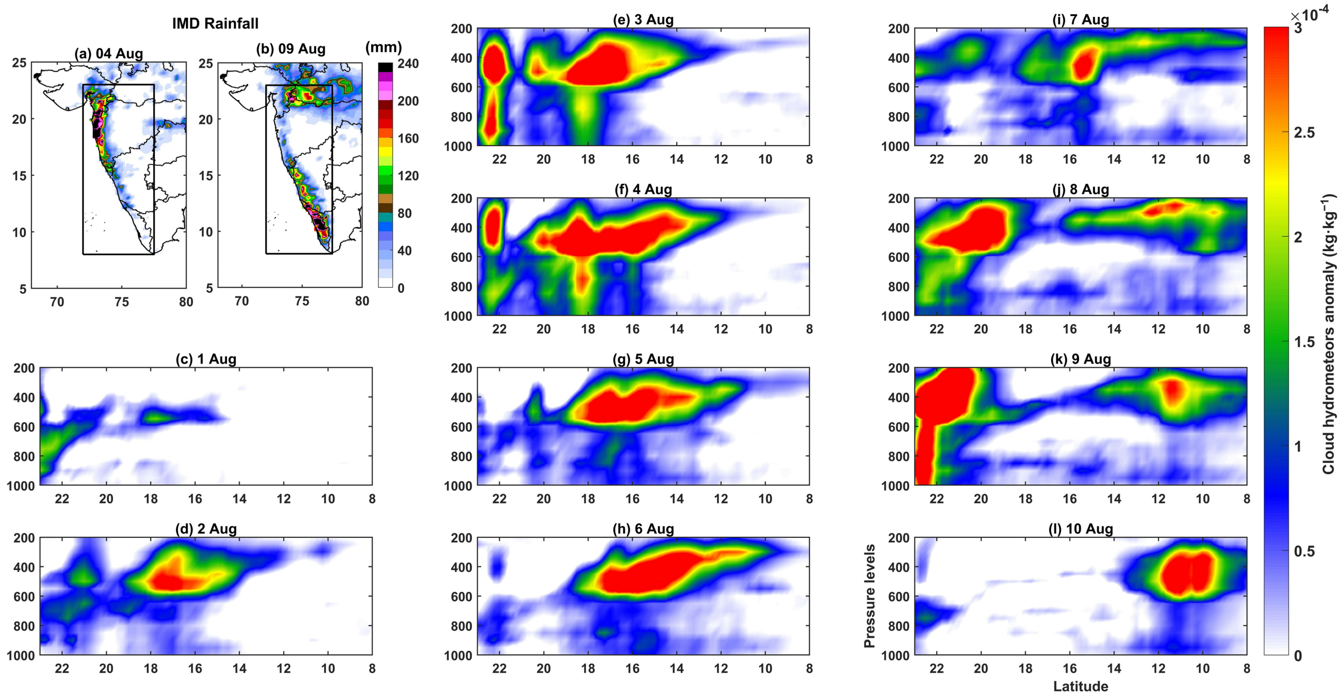

FIGURE 12 (a, b) The IMD rainfall of August 4 and 9, 2019. (c–l) Cloud hydrometeors anomaly (kg/kg) plotted along latitude and pressure level, average over longitude in the selected box 72°–77.5°E in longitude and 8°–23°N in latitude. Cloud hydrometeors cumulative content of cloud liquid water (CLWC), rainwater (RWC), snow water (SWC), and cloud ice (CIWC). [Colour figure can be viewed at wileyonlinelibrary.com]

The positive anomaly in tropospheric temperature (TT), measured in degrees Celsius and averaging between 600 and 200 hPa, is depicted in Figure 11. This elevation in TT signifies a significant release of latent heat by hydrometeors in the upper atmosphere, thereby augmenting the phase conversion of various hydrometeors from one state to another. Examining the temporal evolution, from August 1 to 3 (Figure 11a–c), there is a noticeable intensification of TT over Gujarat, Maharashtra, and a portion of Goa in comparison to its 35-year climatology. Subsequently, on August 4–5 (Figure 11d,e), the intensity of TT reaches even higher levels, particularly over Maharashtra. Moving on to the second row of the figure (Figure 11f–j), it becomes evident that TT maintains a consistently elevated status during the period of rainfall over the land region along the Western Ghats. This underscores the persistent influence of high TT values in the atmospheric conditions during the rainy phase, especially in the vicinity of the Western Ghats. Vaid and San Liang (2015, 2018) demonstrated a strong correlation between TT and precipitation variability across South and East Asia.

The positive anomaly in cumulative cloud hydrometeors (measured in kg·kg^{-1}) across a designated region (depicted in Figure 12a,b) is illustrated in Figure 12c–l, showcasing variations along latitude and pressure levels, while averaging along longitude. The concentration of hydrometeors includes the cumulative content of cloud liquid water (CLWC), rainwater (RWC), snow water (SWC), and cloud ice (CIWC). It has been observed that there is an evident association between elevated VV (as depicted in Figure 9e,f) and TT (illustrated in Figure 11c,d) with the mass of cloud hydrometers. Specifically, during the period of August 3–4 (Figure 12e,f), an increased concentration of cloud hydrometers is observed within the 23°–17°N latitude range, spanning the regions of south Gujarat and Maharashtra. Following this temporal pattern, the concentration of cloud hydrometeors has shifted from higher to lower latitudes, notably between 18°N and 13°N latitude over Goa and Karnataka on August 5–6 (Figure 12g,h). This spatial shift suggests a dynamic movement of atmospheric phenomena, possibly influenced by the identified high VV and TT conditions. In the subsequent timeframe after August 7, a noteworthy accumulation of cloud hydrometeors is observed over the Kerala region. This observation implies a persistence or intensification of atmospheric activity in this specific geographic area. Khadke and Pattnaik (2021) conducted a modelling study revealing high concentrations of cloud hydrometeors during the extreme precipitation event that occurred over Kerala in 2019. Chakraborty et al. (2021) and Ganjir et al. (2022) also highlighted that extreme

10970088, 2024, 13, Downloaded from https://rmets.onlinelibrary.wiley.com/doi/10.1002/joc.8610 by University Of New South Wales, Wiley Online Library on [28/04/2025]. See the Terms and Conditions (https://onlinelibrary.wiley.com/terms-and-conditions) on Wiley Online Library for rules of use; OA articles are governed by the applicable Creative Commons License

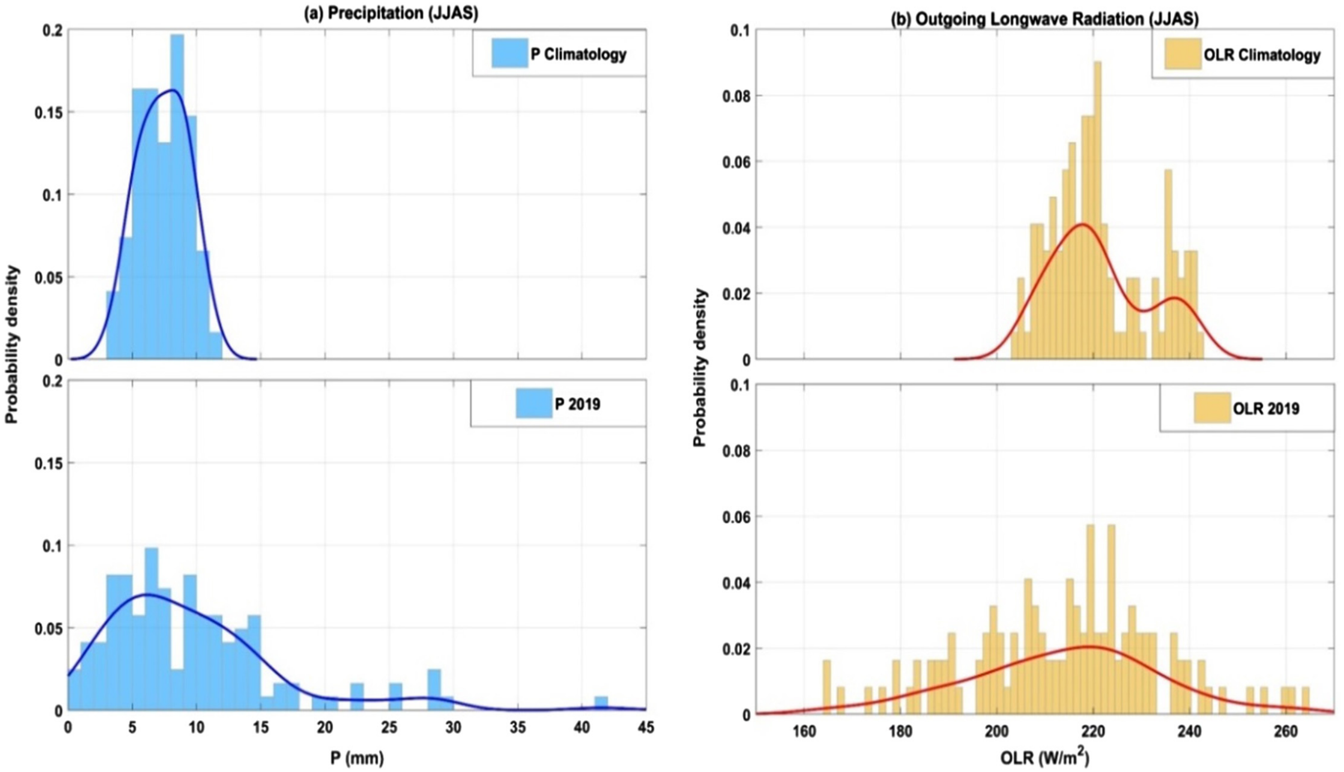

FIGURE 13 (a) Histograms and probability density of rainfall (mm·day^{-1}) over the Western Ghats region (lon: 72°–77.5°E; lat: 8°–23°N) from IMD data for the monsoon season (JJAS). The probability density of outgoing longwave radiation (OLR, W·m^{-2}) over a region (lon: 70°–77.5°E; lat: 8°–23°N) from NOAA. [Colour figure can be viewed at wileyonlinelibrary.com]

rainfall events in the Kerala region are primarily influenced by cloud hydrometeors. Further, we observed the influence of VV and TT on the distribution of cloud hydrometeors, revealing distinct patterns in both time and space. The shifting concentrations along latitudinal bands suggest a dynamic interplay of atmospheric conditions, contributing to the overall understanding of regional meteorological phenomena.

On the other hand, SST leading precipitation when the atmosphere is forced by SSTs (Wu et al., 2008). The warm SST helps to produce more moisture (supersaturation due to more RH) and stronger north–south tropospheric temperature gradient support bringing the moisture over land, which is manifested in the formation of rain through stronger condensation and the Bergeron-Findension process. The less OLR (deep convection) over Gujarat and the West coast from August 2 to August 9 assisted the growth of the cloud hydrometeors (Figure 12), which might be converted to surface rainfall by wet scavenging. The significant subsidence (wet scavenging) is noticed on August 9th–10th over Gujarat and produces more rainfall (Figure 12). Due to the lead–lag relationships between precipitation and SST at intraseasonal timescale heavy precipitation happened on August 9–10th over Gujrat.

We have also computed the probability density of rainfall and OLR in this study (Figure 13). The probability density functions (PDFs) are computed based on the daily climatology of JJAS rainfall (122 days) and the rainfall data from 2019. We used the ksdensity function of MATLAB to overlay the PDF onto the histogram. The probability density of rainfall over the Western Ghats reveals that climatologically (1984–2018) the rain bins of 0–12 mm·day^{-1} dominate during the monsoon season. The higher intensity rainfall events, which represent the tail of the probability density function (PDF) are observed particularly during the extreme rainfall events (Figure 13a) in 2019 (August 1–10, 2019), which are important for the daily variance of ISM rainfall (Goswami & Goswami, 2017). Therefore, the heavy rainfall (Figure 13a, rainfall bins >15 mm·day^{-1}) encountered over the coastal region of Maharashtra from August 1 to 10, 2019. The heavy rainfall during August 2019 events over the Western Ghats are exceptional as compared to long-term climatology (Figure 13a), which is linked with the prevailing large-scale convection (Figure 13b) supported the occurrence of heavy rainfall. The probability density of OLR over larger region (lon: 65°–80°E, and lat: 0°–25°N) from observation also depicts that the tail (higher OLR bins) and the crest (lower OLR

10970088, 2024, 13, Downloaded from https://rmets.onlinelibrary.wiley.com/doi/10.1002/joc.8610 by University Of New South Wales, Wiley Online Library on [28/04/2025]. See the Terms and Conditions (https://onlinelibrary.wiley.com/terms-and-conditions) on Wiley Online Library for rules of use; OA articles are governed by the applicable Creative Commons License

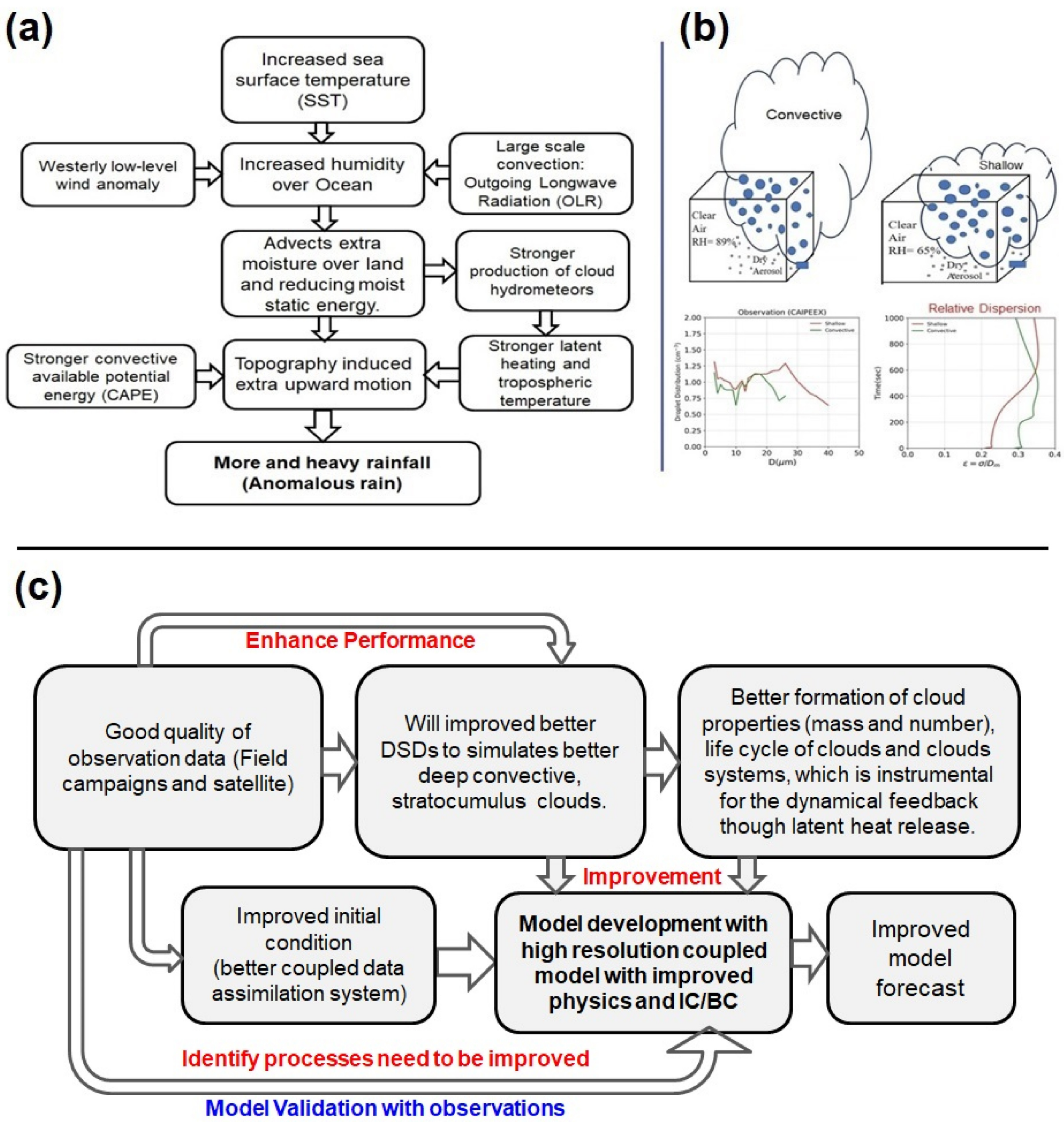

FIGURE 14 (a) Flowchart explains the ocean–atmosphere interactions in the resulting extreme precipitation event. (b) The cloud droplet distributions from in situ airborne observation (CAIPEEX) from shallow and convective clouds are also presented. The calculated relative dispersion from the fundamental theoretical study for shallow and convective clouds (as shown in the schematic) is also portrayed. (c) A conceptual model for the improvement of the model forecast is also presented. [Colour figure can be viewed at wileyonlinelibrary.com]

bin) (Figure 13b) of the OLR PDF significantly different in 2019 August events as compared to long-term climatology. The crest (tail) of the OLR PDF is more (less) during the heavy rainfall events in 2019 as compared to climatology (Figure 13b). The higher (lower) OLR signifies the deep (shallow) convection (Krishnamurti et al., 1989). Therefore, deeper convection during the heavy rainfall events in 2019 (Figure 13b) is responsible for the ample to heavy rain (Figure 13a), which is an important finding and need for the numerical prediction. The histograms of rainfall and OLR are plotted for more clarification of the 2019 event as shown in Figure 13. Our findings indicate significant deep convective clouds, as demonstrated in Figure 13b (with an OLR anomaly of less than $-50\ \mathrm{W{\cdot}m^{-2}}$, as illustrated in Figure 5), coinciding with the heavy rainfall events observed in 2019 (Figure 13a). This is an important finding to demonstrate the need for the correct simulation of convection in numerical prediction models to improve forecasts.

To assess the impact of climate change and shifts in precipitation patterns, we divided the total climatological years into two periods: 1984–2000 and 2001–2018. We then compared these periods with the year 2019 (Figure S2). The present analysis revealed a notable shift

10970088, 2024, 13, Downloaded from https://rmets.onlinelibrary.wiley.com/doi/10.1002/joc.8610 by University Of New South Wales, Wiley Online Library on [28/04/2025]. See the Terms and Conditions (https://onlinelibrary.wiley.com/terms-and-conditions) on Wiley Online Library for rules of use; OA articles are governed by the applicable Creative Commons License

TABLE 1 The quantification of anomalies for meteorological variables and sea surface temperature (SST) for heavy rainfall event.

S. No.	Meteorological variables	Heavy rainfall event
1	Outgoing longwave radiation (OLR)	OLR anomaly $<-50\ \mathrm{W{\cdot}m^{-2}}$
2	Sea surface temperature (SST)	SST anomaly >1.4°C
3	Relative humidity (RH)	RH anomaly >10%
4	Air temperature (TA)	TA anomaly over land ~0.4 to 0.6°C TA anomaly over ocean >1.6°C
5	Wind speed (WS)	WS anomaly $>4\ \mathrm{m{\cdot}s^{-1}}$
6	Vertical velocity (VV)	VV anomaly $>-0.4\ \mathrm{m{\cdot}s^{-1}}$
7	Convective available potential energy (CAPE)	CAPE anomaly $>600\ \mathrm{J{\cdot}kg^{-1}}$
8	Tropospheric temperature (TT)	TT anomaly >1.4°C
9	Cloud hydrometeors (CLWC, CIWC, RWC, and SWC)	Cloud hydrometeors anomaly $>2.5\times10^{-4}\ \mathrm{kg{\cdot}kg^{-1}}$

in precipitation patterns after 2000, indicating a clear signal of climate change that has led to increased rainfall, as shown in Figure S2a. Conversely, observations of OLR indicate an increase post-2000; however, in 2019, the OLR was found to be lower. This suggests that there was enhanced absorption of radiation by both ocean and land, contributing to the trapping of heat.

In summary, our study examined the extreme precipitation event that occurred in 2019 along the southwest coast of India by comparing it with climatological mean over 35 years (1984–2018). The flowchart illustrates the dynamics of meteorological variables, which result the heavy rainfall (Figure 14a). The schematic diagram also demonstrates the variation of cloud droplet size distributions (DSD) from in situ airborne observation, which are important for the modulation of cloud types (from shallow to convective) and relative dispersion calculated from fundamental theoretical study might be helpful to develop a conceptual model to improve quantitative forecast of extreme precipitation using dynamical models (Figure 14). During this event, the OLR and SST were found abnormal which developed a strong ocean-land surface temperature gradient. This disparity in temperature between the ocean and land can create favourable conditions for increased RH in the atmosphere. This moisture is transported through the strong low-level wind (850 hPa) towards land. In this regard, the physically based process understanding from the fundamental theoretical study using the parcel-Bin model is required. The parcel bin model guided by situ observation can shed light on obtaining realistic probability distribution of cloud droplet sizes in shallow and convective clouds. The variation of cloud droplet distributions from shallow to convective clouds is required in the numerical weather prediction model, which can be provided by relative dispersion as shown in the schematic diagram (Figure 14b). The frequencies of shallow and deep convective clouds are related to the relative dispersion (Figure 14b), which can further modify outgoing longwave radiation (OLR). A conceptual model for the improvement of model forecast is also presented (Figure 14c). The quantitative values of meteorological variables and SST anomalies which are plausible causes for the occurrence of extreme precipitation over the Western Ghats are listed in Table 1. The mean anomaly values may vary from event to event.

The table describes quantitatively the anomalies of the important meteorological parameters (thermodynamical, dynamical, and microphysical), which are responsible for triggering the deep convection during the heavy rainfall events over the Western Ghats regions. The strong positive anomaly of SST and TT helps to generate more moisture (source) and propagate to the land regions, which is also reflected in the strong positive anomaly of RH, triggering higher supersaturation and condensations (Table 1). It is also noted that stronger convections as revealed in the strong negative anomaly of OLR and positive anomaly of CAPE manifest in the formation of more cloud hydrometeors as observed in the positive anomaly of cloud hydrometeors (Table 1). This is the first time we have demonstrated the combined interactions among thermodynamics, dynamics, and cloud microphysics to explain the unexplored processes for extreme heavy rainfall events. Earlier most of the heavy rainfall studies were focused on the assessment of dynamics and less emphasis on cloud microphysics.

The rich topography of the region can develop a strong vertical updraft over the Western Ghats. These low-level winds then move vertically upward in the atmosphere where convective available potential energy plays a significant role by providing the amount of energy atmospheric convection. At the same time, the troposphere can act as a heat source to carry and sustain more moisture in the atmosphere by realizing the latent heat through cloud hydrometeors. This condition can increase the moisture-holding capacity of the atmosphere, which subsequently can result in extreme precipitation over this region. The combination of all the above atmospheric dynamics may result in anomalous rainfall

10970088, 2024, 13, Downloaded from https://rmets.onlinelibrary.wiley.com/doi/10.1002/joc.8610 by University Of New South Wales, Wiley Online Library on [28/04/2025]. See the Terms and Conditions (https://onlinelibrary.wiley.com/terms-and-conditions) on Wiley Online Library for rules of use; OA articles are governed by the applicable Creative Commons License

along the coastal regions of Gujarat, Maharashtra, Goa, Karnataka, and Kerala.

It is also important to discuss that orography plays a crucial role in influencing rainfall patterns, especially in regions characterized by complex terrain such as the Western Ghats. Orographic features can enhance rainfall through mechanisms such as orographic lifting, where moist air is forced to ascend over mountains, leading to condensation and vapour depositional growth processes. The thermodynamical phase changes during the cloud processes introduce latent heat release and have an impact on updraft. These processes influence the spatial distribution and intensity of rainfall events across the Western Ghats. The varied elevation and sloping terrain can significantly affect moisture transport, cloud formation, and precipitation distribution. However, the literature suggests that the main source of moisture for precipitation along the western coast of India, particularly the hill regions of the Western Ghats is the ocean. (Pathak et al., 2014; Saranya et al., 2021; Zhang et al., 2021). Ocean-derived moisture predominates over terrestrial sources, and consequently, summer monsoon precipitation dominates over recycled precipitation. Due to this aspect, we have not separately investigated the orographic features in the present study. Moreover, the spatial resolution of the data we used for our study is 25×25 km^2; investigating the orographic features at such coarse resolution would be an imprecise method to interpret the results. This is one of the limitations of our present study and the role of orography on heavy precipitation will be carried out through model sensitivity experiments in future study.

4 | CONCLUSION

In August 2019, the coastal states of southwest India experienced a catastrophic flood situation due to extreme precipitation. The alarming flood situation has severe consequences on society, leading to the loss of lives, livelihoods, properties, and transportation. Southwest India, being a highly vulnerable region, faces annual challenges with erratic precipitation events. Hence, it is crucial to comprehend the dynamics and thermodynamics of such events to enhance nowcasting for improved adaptation. The present study used the ECMWF-ERA5 and IMD rainfall gridded data (0.25° spatial resolution) to analyse this event. We examined the SST, OLR, and other atmospheric variables for 15 days, from July 27 to August 10, 2019, against 35 years of climatological data spanning from 1984 to 2018. In this study, we found that the anomalous precipitation along the Southwest coast of India is a consequence of dynamics, thermodynamics, and cloud microphysics processes. The geographical location, along with atmospheric conditions, was found to be favourable for heavy rainfall over the region, where ocean–atmosphere–land interactions played a significant role. The key conclusions are as follows:

1. Our research highlights the significant influence of warm SST (anomaly >1.40°C), OLR (anomaly <-50 W·m^{-2}), TA (anomaly >1.6°C over ocean) in enhancing the atmospheric moisture holding capacity. This increased moisture, with RH anomalies exceeding 10%, shifts from the ocean to land due to intensified low-level wind (850 hPa), characterized by WS anomalies exceeding 4 m·s^{-1}, and specific flow patterns.
2. The observed moisture increase can be attributed to the significant VV anomaly (>-0.4 m·s^{-1}) and the prevailing atmospheric instability with CAPE anomaly exceeding 600 J·kg^{-1}. The high temperature at tropopause anomaly (>1.4°C) induced warming in the troposphere, leading to the effective melting of cloud hydrometeors. Consequently, this melting process released latent heat, contributing to an increase in the concentration of moisture in the atmosphere.
3. The synergistic influence of cloud hydrometeors, including CLWC, SWC, RWC, and CIWC, exhibiting a noteworthy anomaly surpassing 2.5×10^{-4} kg·kg^{-1}, establishes an ideal setting for the sustained presence of cloud hydrometeors. This complex interplay leads to the result of intense precipitation, underscoring the significance of these atmospheric dynamics in shaping regional weather patterns.

These findings enhance our understanding of the complex relationships among sea-surface conditions, atmospheric moisture dynamics, and wind patterns, revealing their critical role in shaping local precipitation. This can be further elucidated through modelling investigations and in-depth analyses of cloud microphysics and dynamics. The present study describes qualitatively and quantitatively the anomalies of the important meteorological parameters (thermodynamical, dynamical, and microphysical), which are responsible for triggering the deep convection during the heavy rainfall events over the Western Ghats regions. There is ample study of heavy rainfall studies, which are focused on the assessment of dynamics and less emphasis on cloud microphysics. This is the first time we have demonstrated the combined interactions among thermodynamics, dynamics, and cloud microphysics to explain the unexplored processes for extreme heavy rainfall events. This is the novelty of this present study. The strong wind anomaly or cross-equatorial flow over the Arabian Sea helps to produce more sea salt by

10970088, 2024, 13, Downloaded from https://rmets.onlinelibrary.wiley.com/doi/10.1002/joc.8610 by University Of New South Wales, Wiley Online Library on [28/04/2025]. See the Terms and Conditions (https://onlinelibrary.wiley.com/terms-and-conditions) on Wiley Online Library for rules of use; OA articles are governed by the applicable Creative Commons License

bubble burst, which can act as giant condensation nuclei (GCCN) and have an impact on the precipitation through rain embryo formation (microphysical processes). This interaction between dynamical (wind) and cloud microphysics (cloud hydrometeors) is very specific to the particular region of interest. The formation of cloud hydrometeors at lower levels is conducive over the particular region due to the presence of ample sea salt, which can act as rain embryos. The understanding based on the present study can provide a pathway for the future development of the forecast model. The hypothesis based on the present research work and the road map for the numerical model development is also shown here. This innovative research provides direction for the R&D of heavy rainfall prediction.

AUTHOR CONTRIBUTIONS

Leena Khadke: Conceptualization; methodology; formal analysis; data curation; investigation; writing – review and editing; writing – original draft. **Sachin Budakoti:** Investigation; formal analysis; validation; visualization; writing – review and editing; writing – original draft. **Akash Verma:** Investigation; validation; data curation; formal analysis; writing – original draft; writing – review and editing. **Moumita Bhowmik:** Methodology; investigation; validation; formal analysis; visualization; writing – original draft; writing – review and editing. **Anupam Hazra:** Conceptualization; methodology; visualization; formal analysis; supervision; writing – original draft; writing – review and editing.

ACKNOWLEDGEMENTS

The authors express their gratitude to the data agencies maintaining the open-source data utilized in this study, including the European Centre for Medium-Range Weather Forecasts (ECMWF)-ERA5 reanalysis (https://cds.climate.copernicus.eu/#!/search?text=ERA5&type=dataset), the India Meteorological Department (IMD) for rainfall gridded data (https://imdpune.gov.in/cmpg/Griddata/Rainfall_25_Bin.html), and the National Oceanic and Atmospheric Administration (NOAA) for OISST (https://downloads.psl.noaa.gov/Datasets/noaa.oisst.v2.highres/) and OLR (https://www.ncei.noaa.gov/data/outgoing-longwave-radiation-daily/access/). The AH and MB are thankful to the Director, and Project Directors of IITM, for providing encouragement to carry out the research work. The work is part of MTech thesis of the first author carried out at IITM, Pune. The authors are grateful to Editor and two anonymous reviewers for their valuable comments and suggestions.

CONFLICT OF INTEREST STATEMENT

The authors declare no conflicts of interest.

DATA AVAILABILITY STATEMENT

The data that support the findings of this study are available from the corresponding author upon reasonable request.

ORCID

Moumita Bhowmik https://orcid.org/0000-0001-8894-8901

Anupam Hazra https://orcid.org/0000-0002-8658-9412

REFERENCES

Auliya, M.N. & Mulya, A. (2022) Hail identification based on weather factor analysis and Himawari 8 satellite imagery: case study of hail on 2nd March 2021 in Malang Indonesia. *International Journal of Remote Sensing and Earth Sciences*, 18(2), 217–228. Available from: https://doi.org/10.30536/j.ijreses.2021.v18.a3712

Baker, M.B. (1997) Cloud microphysics and climate. *Science*, 276, 1072–1078. Available from: https://doi.org/10.1126/science.276.5315.1072

Bonebrake, T.C. & Mastrandrea, M.D. (2010) Tolerance adaptation and precipitation changes complicate latitudinal patterns of climate change impacts. *Proceedings of the National Academy of Sciences of the United States of America*, 107, 12581–12586. Available from: https://doi.org/10.1073/pnas.0911841107

Budakoti, S. & Singh, C. (2023) Comprehensive study of extreme rainfall events using model simulations and remotely sensed observations. *Hydrological Sciences Journal*, 68, 2317–2335. Available from: https://doi.org/10.1080/02626667.2023.2235349

Chakraborty, T., Pattnaik, S., Jenamani, R.K. & Baisya, H. (2021) Evaluating the performances of cloud microphysical parameterizations in WRF for the heavy rainfall event of Kerala (2018). *Meteorology and Atmospheric Physics*, 133, 707–737. Available from: https://doi.org/10.1007/s00703-021-00776-3

Chaudhari, H.S., Shinde, M.A. & Oh, J.H. (2010) Understanding of anomalous Indian summer monsoon rainfall of 2002 and 1994. *Quatererly International*, 213, 20–32. Available from: https://doi.org/10.1016/j.quaint.2008.05.009

Deegala, D., Song, Y.H., Chung, E.-S., Ayugi, B.O. & Shahid, S. (2023) Future extreme precipitation changes in the South Asian summer monsoon dominance region. *Atmospheric Research*, 295, 107029. Available from: https://doi.org/10.1016/j.atmosres.2023.107029

Field, P.R. & Heymsfield, A.J. (2015) Importance of snow to global precipitation. *Geophysical Research Letters*, 42, 9512–9520. Available from: https://doi.org/10.1002/2015GL065497

Fischer, E.M. & Knutti, R. (2015) Anthropogenic contribution to global occurrence of heavy-precipitation and high-temperature extremes. *Nature Climate Change*, 5, 560–564. Available from: https://doi.org/10.1038/nclimate2617

Fu, D., Guo, X. & Liu, C. (2011) Effects of cloud microphysics on monsoon convective system and its formation environments over the South China Sea: a two-dimensional cloud-resolving modeling study. *Journal of Geophysical Research: Atmospheres*, 116, D07108. Available from: https://doi.org/10.1029/2010JD014662

Gadgil, S., Francis, P.A., Rajendran, K., Nanjundiah, R.S. & Rao, S.A. (2019) Role of land-ocean contrast in the Indian

10970088, 2024, 13, Downloaded from https://rmets.onlinelibrary.wiley.com/doi/10.1002/joc.8610 by University Of New South Wales, Wiley Online Library on [28/04/2025]. See the Terms and Conditions (https://onlinelibrary.wiley.com/terms-and-conditions) on Wiley Online Library for rules of use; OA articles are governed by the applicable Creative Commons License

summer monsoon rainfall. In: *The multiscale global monsoon system. World Scientific series on Asia-Pacific weather and climate*. Singapore: World Scientific, pp. 3–12. Available from: https://doi.org/10.1142/9789811216602_0001

Ganjir, G., Pattnaik, S. & Trivedi, D. (2022) Characteristics of dynamical and thermo-dynamical variables during heavy rainfall events over the Indian region. *Dynamics of Atmospheres and Oceans*, 99, 101315. Available from: https://doi.org/10.1016/j.dynatmoce.2022.101315

Gao, W., Sui, C.-H., Fan, J., Hu, Z. & Zhong, L. (2016) A study of cloud microphysics and precipitation over the Tibetan Plateau by radar observations and cloud-resolving model simulations. *Journal of Geophysical Research: Atmospheres*, 121, 13735–13752. Available from: https://doi.org/10.1002/2015JD024196

Geresdi, I., Rasmussen, R., Grabowski, W. & Bernstein, B. (2005) Sensitivity of freezing drizzle formation in stably stratified clouds to ice processes. *Meteorology and Atmospheric Physics*, 88, 91–105. Available from: https://doi.org/10.1007/s00703-003-0048-5

Goswami, B.B. & Goswami, B.N. (2017) A road map for improving dry-bias in simulating the South Asian monsoon precipitation by climate models. *Climate Dynamics*, 49, 2025–2034. Available from: https://doi.org/10.1007/s00382-016-3439-2

Goswami, B.N., Venugopal, V., Sengupta, D., Madhusoodanan, M.S. & Xavier, P.K. (2006) Increasing trend of extreme rain events over India in a warming environment. *Science*, 314, 1442–1445. Available from: https://doi.org/10.1126/science.1132027

Goswami, B.N. & Xavier, P.K. (2005) ENSO control on the South Asian monsoon through the length of the rainy season. *Geophysical Research Letters*, 32, L18717. Available from: https://doi.org/10.1029/2005GL023216

Hay, J.E. & Williams, P.D. (2023) Drivers of past and future changes in weather, climate and ocean extremes. In: *Science of weather, climate and ocean extremes, developments in weather and climate science*. UK: Elsevier, pp. 195–268. Available from: https://doi.org/10.1016/B978-0-323-85541-9.00012-2

Hazra, A., Chaudhari, H.S. & Dhakate, A. (2016) Evaluation of cloud properties in the NCEP CFSv2 model and its linkage with Indian summer monsoon. *Theoretical and Applied Climatology*, 124, 31–41. Available from: https://doi.org/10.1007/s00704-015-1404-3

Hazra, A., Chaudhari, H.S., Saha, S.K. & Pokhrel, S. (2017) Effect of cloud microphysics on Indian summer monsoon precipitating clouds: a coupled climate modeling study. *Journal of Geophysical Research: Atmospheres*, 122, 3786–3805. Available from: https://doi.org/10.1002/2016JD026106

Hersbach, H., Bell, B., Berrisford, P., Hirahara, S., Horányi, A., Muñoz-Sabater, J. et al. (2020) The ERA5 global reanalysis. *Quarterly Journal of the Royal Meteorological Society*, 146(730), 1999–2049.

Intergovernmental Panel on Climate Change (IPCC). (2023) Weather and climate extreme events in a changing climate. In: *Climate change 2021—the physical science basis: Working Group I contribution to the sixth assessment report of the Intergovernmental Panel on Climate Change*. Cambridge: Cambridge University Press, pp. 1513–1766. Available from: https://doi.org/10.1017/9781009157896.013

Khadke, L. & Pattnaik, S. (2021) Impact of initial conditions and cloud parameterization on the heavy rainfall event of Kerala (2018). *Modeling Earth Systems and Environment*, 7, 2809–2822. Available from: https://doi.org/10.1007/s40808-020-01073-5

Krishnamurti, T.N., Bedi, H.S. & Subramaniam, M. (1989) The summer monsoon of 1987. *Journal of Climate*, 2, 321–340.

Kumar, S., Hazra, A. & Goswami, B.N. (2014) Role of interaction between dynamics, thermodynamics and cloud microphysics on summer monsoon precipitating clouds over the Myanmar coast and the Western Ghats. *Climate Dynamics*, 43, 911–924. Available from: https://doi.org/10.1007/s00382-013-1909-3

Lau, W.K.-M. & Kim, K.-M. (2017) Competing influences of greenhouse warming and aerosols on Asian summer monsoon circulation and rainfall. *Asia-Pacific Journal of Atmospheric Sciences*, 53, 181–194. Available from: https://doi.org/10.1007/s13143-017-0033-4

Lee, M. & Frisius, T. (2018) On the role of convective available potential energy (CAPE) in tropical cyclone intensification. *Tellus A: Dynamic Meteorology and Oceanogrphy*, 70, 1–18. Available from: https://doi.org/10.1080/16000870.2018.1433433

Li, Z. & Yang, S. (2017) Influences of spring-to-summer sea surface temperatures over different Indian Ocean domains on the Asian summer monsoon. *Asia-Pacific Journal of Atmospheric Sciences*, 53, 471–487. Available from: https://doi.org/10.1007/s13143-017-0050-3

Murugavel, P., Pawar, S.D. & Gopalakrishnan, V. (2012) Trends of convective available potential energy over the Indian region and its effect on rainfall. *International Journal of Climatology*, 32, 1362–1372. Available from: https://doi.org/10.1002/joc.2359

Nikumbh, A.C., Chakraborty, A. & Bhat, G.S. (2019) Recent spatial aggregation tendency of rainfall extremes over India. *Scientific Reports*, 9, 10321. Available from: https://doi.org/10.1038/s41598-019-46719-2

Pai, D.S., Rajeevan, M., Sreejith, O.P., Mukhopadhyay, B. & Satbha, N.S. (2014) Development of a new high spatial resolution ($0.25^\circ \times 0.25^\circ$) long period (1901–2010) daily gridded rainfall data set over India and its comparison with existing data sets over the region. *Mausam*, 65, 1–18. Available from: https://doi.org/10.54302/mausam.v65i1.851

Pathak, A., Ghosh, S. & Kumar, P. (2014) Precipitation recycling in the Indian subcontinent during summer monsoon. *Journal of Hydrometeorology*, 15(5), 2050–2066. Available from: https://doi.org/10.1175/JHM-D-13-0172.1

Paul, S., Ghosh, S., Rajendran, K. & Murtugudde, R. (2018) Moisture supply from the Western Ghats forests to water deficit East Coast of India. *Geophysical Research Letters*, 45, 4337–4344. Available from: https://doi.org/10.1029/2018GL078198

Rajeevan, M., Rohini, P., Niranjan Kumar, K., Srinivasan, J. & Unnikrishnan, C.K. (2013) A study of vertical cloud structure of the Indian summer monsoon using CloudSat data. *Climate Dynamics*, 40, 637–650. Available from: https://doi.org/10.1007/s00382-012-1374-4

Rajendran, K., Kitoh, A., Srinivasan, J., Mizuta, R. & Krishnan, R. (2012) Monsoon circulation interaction with Western Ghats orography under changing climate. *Theoretical and Applied Climatology*, 110, 555–571. Available from: https://doi.org/10.1007/s00704-012-0690-2

Raju, A., Parekh, A., Chowdary, J.S. & Gnanaseelan, C. (2015) Assessment of the Indian summer monsoon in the WRF regional climate model. *Climate Dynamics*, 44, 3077–3100. Available from: https://doi.org/10.1007/s00382-014-2295-1

10970088, 2024, 13, Downloaded from https://rmets.onlinelibrary.wiley.com/doi/10.1002/joc.8610 by University Of New South Wales, Wiley Online Library on [28/04/2025]. See the Terms and Conditions (https://onlinelibrary.wiley.com/terms-and-conditions) on Wiley Online Library for rules of use; OA articles are governed by the applicable Creative Commons License

Saranya, P., Krishnakumar, A., Sinha, N., Kumar, S. & Krishnan, K.A. (2021) Isotopic signatures of moisture recycling and evaporation processes along the Western Ghats orography. *Atmospheric Research*, 264, 105863. Available from: https://doi.org/10.1016/j.atmosres.2021.105863

Schmeller, G. & Geresdi, I. (2019) Study of interaction between cloud microphysics and chemistry using coupled bin microphysics and bin aqueous chemistry scheme. *Atmospheric Environment*, 198, 366–380. Available from: https://doi.org/10.1016/j.atmosenv.2018.10.064

Scoccimarro, E., Gualdi, S., Bellucci, A., Zampieri, M. & Navarra, A. (2013) Heavy precipitation events in a warmer climate: results from CMIP5 models. *Journal of Climate*, 26, 7902–7911. Available from: https://doi.org/10.1175/JCLI-D-12-00850.1

Sebastian, D.E., Murtugudde, R. & Ghosh, S. (2023) Soil–vegetation moisture capacitor maintains dry season vegetation productivity over India. *Scientific Reports*, 13, 888. Available from: https://doi.org/10.1038/s41598-022-27277-6

Shahi, N.K., Das, S., Ghosh, S., Maharana, P. & Rai, S. (2021) Projected changes in the mean and intra-seasonal variability of the Indian summer monsoon in the RegCM CORDEX-CORE simulations under higher warming conditions. *Climate Dynamics*, 57, 1489–1506. Available from: https://doi.org/10.1007/s00382-021-05771-3

Tabari, H. (2020) Climate change impact on flood and extreme precipitation increases with water availability. *Scientific Reports*, 10, 13768. Available from: https://doi.org/10.1038/s41598-020-70816-2

Tamoffo, A.T., Weber, T., Akinsanola, A.A. & Vondou, D.A. (2023) Projected changes in extreme rainfall and temperature events and possible implications for Cameroon's socio-economic sectors. *Meteorological Applications*, 30, e2119. Available from: https://doi.org/10.1002/met.2119

Trenberth, K.E. (2011) Changes in precipitation with climate change. *Climate Research*, 47, 123–138. Available from: https://doi.org/10.3354/cr00953

UNESCO World Heritage Centre. (2024) Western Ghats. Available from: https://whc.unesco.org/en/list/1342/#:~:text=A%20chain%20of%20mountains%20running,%2C%20Goa%2C%20Maharashtra%20and%20Gujarat [Accessed on 2nd June 2024].

Vaid, B.H. & San Liang, X. (2015) Tropospheric temperature gradient and its relation to the South and East Asian precipitation variability. *Meteorology and Atmospheric Physics*, 127, 579–585. Available from: https://doi.org/10.1007/s00703-015-0385-1

Vaid, B.H. & San Liang, X. (2018) An abrupt change in tropospheric temperature gradient and moisture transport over East Asia in the late 1990s. *Atmosphere-Ocean*, 56, 268–276. Available from: https://doi.org/10.1080/07055900.2018.1429381

Varikoden, H., Revadekar, J.V., Kuttippurath, J. & Babu, C.A. (2019) Contrasting trends in southwest monsoon rainfall over the Western Ghats region of India. *Climate Dynamics*, 52, 4557–4566. Available from: https://doi.org/10.1007/s00382-018-4397-7

Verma, A., Chandel, V. & Ghosh, S. (2022) Climate drivers of the variations of vegetation productivity in India. *Environmental Research Letters*, 17, 084023. Available from: https://doi.org/10.1088/1748-9326/ac7c7f

Vinayachandran, P.N., Shankar, D., Kurian, J., Durand, F. & Shenoi, S.S.C. (2007) Arabian Sea mini warm pool and the monsoon onset vortex. *Current Science*, 93, 203–214.

Wu, R., Kirtman B.P. & Pegion, K. (2008) Local rainfall–SST relationship on subseasonal time scales in satellite observations and CFS. *Geophysical Research Letters*, 35, L22706.

Wu, Q.-Y., Li, Q.-Q., Ding, Y.-H., Shen, X.-Y., Zhao, M.-C. & Zhu, Y.-X. (2022) Asian summer monsoon responses to the change of land–sea thermodynamic contrast in a warming climate: CMIP6 projections. *Advances in Climate Change Research*, 13, 205–217. Available from: https://doi.org/10.1016/j.accre.2022.01.001

Zhang, S., Liu, B., Ren, G., Zhou, T., Jiang, C., Li, S. et al. (2021) Moisture sources and paths associated with warm-season precipitation over the Sichuan Basin in southwestern China: climatology and interannual variability. *Journal of Hydrology*, 603, 127019. Available from: https://doi.org/10.1016/j.jhydrol.2021.127019

SUPPORTING INFORMATION

Additional supporting information can be found online in the Supporting Information section at the end of this article.

How to cite this article: Khadke, L., Budakoti, S., Verma, A., Bhowmik, M., & Hazra, A. (2024). Examining the evolution of extreme precipitation event using reanalysis and the observed datasets along the Western Ghats. *International Journal of Climatology*, *44*(13), 4829–4847. https://doi.org/10.1002/joc.8610

10970088, 2024, 13, Downloaded from https://rmets.onlinelibrary.wiley.com/doi/10.1002/joc.8610 by University Of New South Wales, Wiley Online Library on [28/04/2025]. See the Terms and Conditions (https://onlinelibrary.wiley.com/terms-and-conditions) on Wiley Online Library for rules of use; OA articles are governed by the applicable Creative Commons License